Published in final edited form as:
Cell Metab. 2008 August ; 8(2): 118–131. doi:10.1016/j.cmet.2008.06.005.

Neural and Molecular Dissection of a *C. elegans* Sensory Circuit that Regulates Fat and Feeding

Elisabeth R. Greer[1], **Carissa L. Perez**[2,3], **Marc R. Van Gilst**[2], **Brian H. Lee**[1], and **Kaveh Ashrafi**[1,*]

1 *Department of Physiology, 600 16th Street, Mission Bay Campus Box 2240, University of California, San Francisco, California, 94158-2517*

2 *Division of Basic Sciences, Fred Hutchinson Cancer Research Center, Seattle, WA 98109*

3 *Molecular and Cellular Biology Program, University of Washington, Seattle, WA 98195*

Summary

A major challenge in understanding energy balance is deciphering the neural and molecular circuits that govern behavioral, physiological and metabolic responses of animals to fluctuating environmental conditions. The neurally expressed TGF-β ligand DAF-7 functions as a gauge of environmental conditions to modulate energy balance in *C. elegans*. We show that *daf-7* signaling regulates fat metabolism and feeding behavior through a compact neural circuit that allows for integration of multiple inputs, and the flexibility for differential regulation of outputs. Perception of depleting food resources in *daf-7* mutants causes fat accumulation despite reduced feeding rate. This fat accumulation is mediated, in part, through neural metabotropic glutamate signaling and upregulation of peripheral endogenous biosynthetic pathways that direct energetic resources into fat reservoirs. Thus, neural perception of adverse environmental conditions can promote fat accumulation without a concomitant increase in feeding rate.

Introduction

Animals respond to changes in food availability through coordinated behavioral, physiological, and metabolic responses. In mammals, the central nervous system (CNS) integrates internal and external signals of energy demand and availability and coordinates outputs ranging from feeding behavior and energy expenditure (Douglas et al., 2005; Morton et al., 2006; Saper et al., 2002). The identities and organization of neural circuits that regulate energy balance are just beginning to be elucidated (Elmquist et al., 1998; Morton et al., 2006; Sternson et al., 2005; Volkow and Wise, 2005). These circuits have largely been proposed based on a combination of gene expression studies, neuroanatomy, electrophysiology and imaging techniques. Recently, brain region specific gene activation and inactivation studies have begun to test and challenge the physiological significance of some these proposed neurocircuits (Balthasar et al., 2004; Balthasar et al., 2005; de Luca et al., 2005; Dhillon et al., 2006; Fulton et al., 2006; Hommel et al., 2006). However, the enormous complexity of the mammalian nervous system makes functional dissection of neural circuits a daunting task. In addition to internal signals of energy availability, visual, olfactory, gustatory, and other sensory cues also

* Corresponding author Kaveh Ashrafi, Ph: 415-514-4102, Fax: 415-514-4242, E-mail: kaveh.ashrafi@ucsf.edu.

act on the CNS to modulate feeding behavior (Volkow and Wise, 2005). Little is known about the molecular and neural circuits that underlie perception of environmental conditions and their interplay with mechanisms that govern behavioral, physiological, and metabolic pathways.

The relative simplicity of the *C. elegans* nervous system offers the opportunity to functionally dissect the genetic and neural basis of food-evoked responses at great resolution. Several lines of evidence indicate that, as in mammals, changes in nutrient availability elicit myriad behavioral, physiological, and metabolic responses in *C. elegans*. For instance, removal of *C. elegans* from their food source, bacterial lawns, causes a ~50% reduction in feeding rate, which is, upregulated upon re-introduction to food (Avery and Horvitz, 1990). *C. elegans* feeding rate is measured by the number of contraction-relaxation cycles, pumps, exhibited by the pharyngeal muscle, the worm's feeding organ (Avery, 1993b). When re-exposed to food, starved animals temporarily feed faster than well-fed animals (Avery and Horvitz, 1990). Thus, *C. elegans* feeding rate is not a simple reflex to food but can be entrained by the experience of starvation. Upon food depletion, hermaphrodites retain eggs (Trent, 1982), are less likely to mate with males (Lipton et al., 2004), and initiate various foraging behaviors (Hills et al., 2004; Sawin et al., 2000). *C. elegans* also respond to dietary change and starvation through alterations in expression of fat metabolic genes (Taubert et al., 2006; Van Gilst et al., 2005a; Van Gilst et al., 2005b) composition of fat stores (Brock et al., 2007; Van Gilst et al., 2005b), and depletion of fat reservoirs (McKay et al., 2003). How this wide range of responses are coordinated and molecularly relate to each other are poorly understood.

We investigated the signaling cascade initiated by the TGF-β like ligand DAF-7 as a potential neural sensory mechanism coordinating energy balance in response to fluctuating environmental conditions. DAF-7 and its downstream signaling cascade were first identified in the context of dauer formation, an alternative developmental stage akin to hibernation (Riddle, 1997; Wadsworth and Riddle, 1989). When faced with low food availability, high population density and high temperature, early larval stage animals halt development and enter the hibernating dauer stage. Like hibernating mammals, dauer larvae are generally non-motile, non-feeding, and contain large fat reservoirs (Riddle, 1997; Wadsworth and Riddle, 1989). Dauer stage animals display metabolic (O'Riordan and Burnell, 1989; Wadsworth and Riddle, 1989), and gene expression changes (Wang and Kim, 2003) that favor utilization of stored fats suggesting that fat reservoirs function as a nutrient source for these non-feeding animals.

daf-7 gene expression is only detected in one pair of sensory neurons named ASI (Ren et al., 1996; Schackwitz et al., 1996). Absence of food or excess daumone, a constitutively secreted pheromone (Butcher et al., 2007; Jeong et al., 2005; Ren et al., 1996) through which *C. elegans* gauge population density, reduce *daf-7* expression leading to dauer formation (Ren et al., 1996; Schackwitz et al., 1996). Accordingly, *daf-7* loss of function promotes constitutive dauer formation even under favorable food condition and low population density (Ren et al., 1996; Riddle, 1997). Exposure of dauers to food results in re-expression of *daf-7*, resumption of feeding and reproductive growth (Ren et al., 1996). Thus, the *daf-7* pathway functions as a sensor of environmental conditions to determine whether larval stage animals grow reproductively or enter hibernation.

Here, we report that the *daf-7* signaling pathway is not restricted to development but funcions generally as a neural sensory gauge of environmental conditions to modulate various energy balance pathways including feeding behavior, fat metabolism and reproduction in adult animals. Interestingly, down-regulation of *daf-7*, which reflects depleting nutrient conditions, causes build-up of fat reservoirs despite reduced feeding rate. To understand this inverse relationship between fat accumulation and feeding rate, we identified neurons and pathways that mediate *daf-7* regulation of these processes. Although receptors for DAF-7 are broadly expressed, we found that signaling from the ASI sensory neurons to only two pairs of

interneurons, RIM and RIC, was sufficient for wild-type growth, egg laying, fat, and feeding rate. In turn, we found that distinct signaling cascades are initiated in these interneurons to independently modulate fat and feeding. *daf-7* inactivation leads to fat accumulation, in part, through enhanced endogenous fat biosynthesis. Therefore, despite reduced feeding rate, available energetic resources are preferentially targeted to fat reservoirs, an adaptive response consistent with perception of depleting nutrient resources. The organizational logic of the neurocircuitry revealed in our analyses allows for integration of multiple inputs and differential regulation of outputs indicating that fat and feeding are coordinated by independent outputs of the nervous system.

Results

Reduced DAF-7 Signaling Causes Excess Fat Despite Reduced Feeding

DAF-7/TGF-β ligand signals through the type I and type II TGF-β receptors DAF-1 and DAF-4 (Estevez et al., 1993; Georgi et al., 1990). Signaling through DAF-1/DAF-4 receptors inactivates DAF-3, a receptor associated co-SMAD, to block dauer entry and promote reproductive growth (Patterson et al., 1997). Dauer promoting activity of DAF-3 is, in turn, dependent on DAF-12, a nuclear hormone receptor (Antebi et al., 2000) (Figure 1A). At 25° C, loss of function mutations in *daf-7*, *daf-1*, and *daf-4* cause constitutive dauer entry while loss of function mutations in *daf-3* and *daf-12* abrogate dauer entry (Riddle, 1997).

When maintained at 20°C *daf-7*, *daf-1*, and *daf-4* mutants grew into reproductive adults that displayed feeding rates that were reduced by ~20–25% relative to wild-type hermaphrodites (Figure 1B and Table S1). Similar to dauers (Kimura et al., 1997), late larval and early adult stage *daf-7*, *daf-1* and *daf-4* mutants accumulated ~2.5 fold more fat relative to wild type (Figures 1C–D, 5B–C, and data now shown). As previously reported (Trent, 1982), all of these mutants also retained eggs (examples shown in Figure S1). The high fat, egg retention and reduced feeding phenotypes *daf-7* and *daf-1* were dependent on *daf-3* (Figure 1B–D and data not shown). By contrast, loss of *daf-12* did not alter the excess fat, reduced feeding, and egg retention rates of these mutants (Figure 1B–D and data not shown). Thus, while both *daf-3* and *daf-12* are required for dauer entry when *daf-7* or *daf-1* are inactivated, fat, feeding, and egg retention phenotypes of these mutants only require *daf-3*. This suggests a molecular divergence in regulation of dauer entry from mechanisms that regulate fat, feeding, and egg retention.

daf-7 Functions as an Environmental Sensor in Adults

We sought to distinguish whether the excess fat and reduced feeding phenotypes of *daf-7* and *daf-1* mutants were due to altered development or reflected an adult sensory role for this pathway. Exposure of well-fed, wild-type adults to an acute 2 hr. dauer pheromone treatment caused a 15% reduction in feeding rate, mimicking the rate of untreated *daf-7* mutants (Figure 1B). Under similar conditions, pheromone treatment did not alter the already reduced feeding rates of *daf-7* and *daf-1* mutants or change the wild-type feeding rate of *daf-3* mutants (Figure 1B) suggesting that inhibition of DAF-7/DAF-1 signaling and subsequent activation of DAF-3 underlie the reduced feeding caused by acute pheromone treatment. Finally, *daf-12* mutants were susceptible to pheromone-induced feeding reduction further supporting the notion that *daf-12* is required for dauer formation but not other *daf-7*-regulated processes. This short pheromone treatment did not elicit detectable changes in fat content and egg retention in any of the genotypes tested (data not shown).

To examine the consequences of reactivating *daf-1* in late larval/early adult stage *daf-1(−)* mutants, we generated transgenic *daf-1(−)* animals carrying full length *daf-1* under the control of a ubiquitously expressed heat-shock activated promoter, *hsp16.2* (Bacaj and Shaham, 2007; Stringham et al., 1992). Fat, feeding, and egg retention phenotypes of these transgenic

animals grown to the young adult stage without heat-shock were indistinguishable from *daf-1 (−)* mutants (Figure 1D–E and data not shown). By contrast, transgenic animals that were briefly heat-shocked at the L3/early L4 stage, displayed nearly wild-type fat, feeding, and egg retention phenotypes within 24 hours (Figure 1C–E and data not shown). Consistent with acute pheromone treatment results, heat-shocked transgenic animals displayed nearly wild-type feeding rates as early as 30 minutes post treatment (Figure 1E) while reversal of fat content and egg retention phenotypes took up to 24 hours.

We also examined feeding rates of food deprived adult-stage wild type and *daf-7* pathway mutants. Within ~1 hr. of food deprivation, wild type and all mutant genotypes displayed similar feeding rates (~50% of rate of well-fed wild-type animals) (Figure 1B). Thus, inactivation of *daf-7/daf-1* signaling does not shift basal feeding rates. Together, these findings suggest that the *daf-7* pathway has an environmental sensory role in late larval and early adult stage animals and that phenotypes associated with inactivation of this pathway are not merely consequences of altered development.

Genetic Dissection of DAF-7 Neurocircuitry of Fat and Feeding

Since *C. elegans* reduce their feeding rate with decreasing food concentrations (Avery and Horvitz, 1990), the reduced feeding of *daf-7* mutants is consistent with perception of increased population density and depleting food resources. Similar to fat accumulation in preparation for dauer entry (John, 2005; Kimura et al., 1997; Wadsworth and Riddle, 1989), adult stage build-up of fat reservoirs and retention of eggs is also consistent with preparations for periods of nutrient deprivation (John, 2005; Kimura et al., 1997; Wadsworth and Riddle, 1989). This, however, raises the perplexing question of how, despite a ~25% reduction in feeding rate, *daf-7* and *daf-1* mutants accumulate some of the greatest fat reservoirs observed in *C. elegans* (Kimura et al., 1997; Sze et al., 2000). To understand the perplexing relationship between fat and feeding in *daf-7* and *daf-1* mutants, we next sought to determine cellular sites through which *daf-7* signaling modulates fat and feeding.

While *daf-7* expression is restricted to the pair of ASI sensory neurons, its receptors, *daf-1* and *daf-4*, are broadly expressed (Gunther et al., 2000). *daf-1* is expressed in pharyngeal neurons, ciliated sensory neurons, interneurons, ventral nerve cord neurons, and in distal tip cells of the gonad. *daf-4* expression overlaps with *daf-1* expression but also extends to other cells and tissues (Gunther et al., 2000). We focused on cells that express the DAF-1 receptor for three reasons. First, *daf-1(−)* fat, feeding, egg retention, and growth phenotype are indistinguishable from corresponding *daf-7(−)* phenotypes. Second, although the *C. elegans* genome expresses several TGF-β type ligands, thus far, the DAF-1 receptor has only been implicated in DAF-7 signaling (Krishna et al., 1999). Third, inactivation of *sma-6*, encoding the only other type I receptor identified in the *C. elegans* genome, causes small body size but is not associated with changes in feeding rate and fat (Table S1 and data not shown).

To identify cells that require *daf-1* signaling for wild-type regulation of feeding, fat storage, egg retention and dauer formation, we expressed full-length *daf-1* using 20 different neuron-specific promoters in *daf-1(−)* mutant animals. For each promoter, we generated a full length *daf-1::gfp* fusion and a corresponding *promoter::gfp* reporter. For each construct, we generated multiple independent transgenic lines (3 on average for each *promoter::daf-1::gfp*). Gene expression was confirmed by observing appearance of GFP in target cells (examples in Figure 2A). The results described below and summarized in Table 1 were consistent across multiple independent lines.

Expression of *daf-1::gfp* under its own promoter or the *egl-3* pan-neural promoter fully rescued the adult feeding rate (Table 1, Figure 2B), fat storage (Figures 2C and S2), egg retention, and larval dauer phenotypes of *daf-1(−)* animals (Table 1, examples of dauers and egg retention

phenotypes are shown in Figure S2). We then systematically targeted *daf-1::gfp* to sensory, inter-, and pharyngeal neurons. Reconstitution of *daf-1* in ASI neurons alone, site of *daf-7* expression, or in almost all 60 ciliated sensory neurons using the *bbs-1* and *osm-6* promoters (Ansley et al., 2003;Collet et al., 1998), failed to rescue any of the *daf-1(−)* phenotypes (Table 1,Figures 2B–C and S2, and data not shown). Reconstitution of *daf-1* in pharyngeal neurons or gland cells using *glr-7, glr-8* (Brockie et al., 2001a) and B0280.7 promoters also failed to rescue any of the *daf-1(−)* phenotypes (Table 1,Figure 2B, and data not shown). By contrast, directing *daf-1::gfp* expression by *glr-1, glr-4*, and *glr-5* promoters (Brockie et al., 2001a), which target interneurons, fully reverted the dauer formation, egg-laying, feeding rate and fat storage phenotypes of *daf-1(−)* mutants back to wild-type levels (Table 1,Figures 2B–C and S2). However, expression of *daf-1::gfp* under the *glr-2* promoter, which targets 24 interneurons, or the *unc-47* and *unc-17* promoters (Alfonso et al., 1993;Eastman et al., 1999), which target the 29 GABAergic and the 80 acetylcholinergic motor neurons, respectively, did not alter various *daf-1(−)* mutant phenotypes (Table 1 and data not shown). Thus, *daf-1* expression in a specific subset of interneurons is sufficient to allow for normal development, egg laying, pumping rate, and fat storage. This is consistent with the role of interneurons as integrators of sensory information.

DAF-7 Signals to RIM and RIC Interneurons To Regulate Fat and Feeding

We asked whether reconstitution of *daf-1* in only a subset of interneurons targeted by the rescuing *glr-1*, *glr-4*, and *glr-5* promoters would be sufficient to restore wild-type fat, feeding, growth, and egg-retention to *daf-1* mutants. We reconstituted *daf-1::gfp* expression under each of *glr-2, ggr-1, dop-1*, *nmr-2*, and *flp-1* promoters (Brockie et al., 2001a; Tsalik et al., 2003) which direct expression to various subsets of cells also targeted by *glr-5, glr-4*, and *glr-1* rescuing constructs (Table S2). *daf-1(−)* phenotypes were fully rescued when *daf-1::gfp* expression was directed by *nmr-2* but not by *glr-2, ggr-1, flp-1, or dop-1* promoters (Table 1 and data not shown). Expression of *glr-5, glr-4, glr-1*, and *nmr-2* promoters compared to all other tested promoters pointed to the RIM pair of interneuron as the only cells commonly targeted by these rescuing promoters and absent in all non-rescuing promoters (Table S2). This was possible since we could verify expression patterns of various promoters in anatomically identifiable neurons (Table S2).

To test the role of RIM in *daf-1* signaling, we used a *tdc-1* promoter targeting gene expression to only two pairs of interneurons, RIM and RIC, as well as the UV-1 uterine–vulval cells (Alkema et al., 2005). All *daf-1(−)* phenotypes were fully rescued when *daf-1::gfp* expression was directed by this promoter (Table 1, Figures 2B–C, S2 and data not shown). Exclusive expression of *daf-1::gfp* in RIC interneurons by a *tbh-1* promoter also restored wild-type fat but only partially rescued the reduced feeding and dauer constitutive phenotypes of *daf-1(−)* (Table 1, Figures 2B–C and S2). Unlike the *tdc-1* promoter, this *tbh-1* promoter did not rescue egg retention phenotype of *daf-1(−)* animals (data not shown). To demonstrate that RIM and RIC are normally recipients of the DAF-7 signal, we expressed $P_{tdc\text{-}1}$*::RFP* and a functional $P_{daf\text{-}1}$*::daf-1::gfp* and noted a clear overlap between these reporter-fusions in RIM and RIC (Figure 2D). Consistent with a previous report (Gunther et al., 2000), *daf-1* expression was not detectable in UV-1 cells suggesting that these cells are not physiological targets of DAF-7.

These data strongly suggest that the site of *daf-1* expression, specifically in RIM and RIC, rather than extent of *daf-1* expression determine whether wild-type fat, feeding, and reproduction levels are restored to *daf-1(−)* animals. Moreover, since ASI does not synapse onto either RIM or RIC, our data indicate that DAF-7 peptidergic signaling is not confined by direct synaptic connections.

Selective Activation of *daf-3* in RIM and RIC Interneurons

Since DAF-1 signaling antagonizes activity of the co-SMAD DAF-3, we asked whether selective activation of DAF-3 in RIM and RIC interneurons could lead to growth, fat, feeding, or egg retention phenotypes. Full length *daf-3* was expressed using *daf-1, osm-6, glr-7, tdc-1,* and *tbh-1* promoters in *daf-1(−); daf-3(−)* double mutants. In this background, targeted cells would gain DAF-3 activity since the inhibitory function of DAF-1 is eliminated. Selective reconstitution of *daf-3* in ciliated sensory and pharyngeal neurons using the *osm-6* and *glr-7* promoters, respectively, did not alter the fat and feeding rates of *daf-1(m40); daf-3(mgDf90)* animals (Figure 3A–C). By contrast, reconstitution using the *tdc-1* promoter resulted in reduced feeding rate and increased fat levels similar in magnitude to those seen when *daf-3* was broadly expressed using the *daf-1* promoter (Figure 3A–C). Furthermore, up to ~20% of animals in which *daf-3* was reconstituted in only RIM and RIC formed dauers (Table S3). This is a significant percentage since broad neuronal expression of *daf-3* caused dauer formation in only ~40% of transgenic animals. Finally, selective reconstitution of *daf-3* in RIC interneuron alone was insufficient to alter the fat and feeding phenotypes of *daf-1(−); daf-3(−)* animals. These findings supported the *daf-1* reconstitution studies in showing that regulation of fat and feeding in response to the environmentally-sensitive DAF-7 signal is funneled through RIM and RIC.

Inactivation of *daf-7* Reduces Feeding Via Neurotransmitters Tyramine and Octopamine

RIM and RIC are somatic nerve interneurons located in the lateral ganglion (White et al., 1986). RIM functions as a motor neuron and links the *C. elegans* tactile-responsive locomotory neural circuit to the neural circuit that regulates head movements. RIC is the sole cellular site for synthesis of the monoamine neurotransmitter octopamine (Alkema et al., 2005). Synthesis of tyramine and octopamine requires conversion of tyrosine to tyramine by tyrosine decarboxylase (TDC-1*)* and subsequent conversion of tyramine to octopamine by tyramine β-hydroxylase (TBH-1). RIM synthesizes tyramine but not octopamine while RIC can synthesize both tyramine and octopamine (Alkema et al., 2005). Other neurons do not synthesize either of these neurotransmitters.

Exogenous tyramine or octopamine were previously shown to reduce pharyngeal pumping rates (Horvitz et al., 1982). Treatment of wild-type animals with exogenous tyramine or octopamine caused reduced feeding reminiscent of rates of *daf-7* or *daf-1* mutants while loss of function of either *tdc-1* or *tbh-1* restored nearly wild-type feeding rate to *daf-1* and *daf-7* mutants (Figure 4A). These data suggested that active *daf-7/daf-1* signaling regulates feeding by blocking tyraminergic and octopaminergic transmissions that originate in RIM and RIC.

To further delineate the *daf-7* feeding regulatory pathway, we examined feeding rates of *ser-2* and *tyra-2* mutants. *ser-2* and *tyra-2* encode two *C. elegans* biogenic G-protein coupled receptors that exhibit greatest *in vitro* binding affinity for tyramine (Rex et al., 2005; Rex et al., 2004). *ser-2(−)* and *tyra-2(−)* mutants had wild-type feeding rates, however, inactivation of *ser-2* but not *tyra-2* restored wild-type feeding rate to *daf-1* mutants (Figure 4A and Figure S3). This was consistent with previous characterization of *ser-2* as a tyraminergic receptor that modulates feeding (Rex and Komuniecki, 2002; Rex et al., 2004). To demonstrate that tyramine signaling through the SER-2 receptor modulates feeding in response to environmental cues, *tdc-1(−)* and *ser-2(−)* adults were acutely treated with pheromone. Unlike wild-type animals, pheromone treatment did not alter the feeding rates of these mutants (Figure S3). Additionally, in response to starvation, *tdc-1(−)* and *ser-2(−)* mutants did not exhibit the full extent of feeding reduction seen in wild-type animals (Figure S3).

To determine cellular sites where *ser-2* signaling elicits feeding rate reduction, we selectively reconstituted *ser-2* in *daf-1(−);ser-2(−)* double mutants. *ser-2* expression has been reported in ~10% of head neurons, head muscle, and pharyngeal neurons (Tsalik et al., 2003). Selective

reconstitution of *ser-2* in pharyngeal muscle using the *myo-2* promoter (Okkema PG et al., 1993) did not alter the feeding rate of *daf-1(−); ser-2(−)* (Figure 4F). Only a modest reduction in feeding rate was obtained when an *egl-3* promoter was used to broadly express *ser-2* in head neurons but only weakly in pharyngeal neurons (Figure 4D). By contrast, *ser-2* reconstitution using a *glr-7* promoter was sufficient to reduce feeding rate of *daf-1(−); ser-2(−)* double mutants down to the rate of *daf-1(−)* (Figure 4D). *glr-7* promoter targets expression to I1, I2, I3, and I6 pharyngeal interneurons, M1 pharyngeal neuron, and NSM neurosecretory motoneurons (Brockie et al., 2001a). Some of these neurons have previously been implicated in regulation of pharyngeal muscle pumping (Avery, 1993a; Avery and Horvitz, 1989; Niacaris and Avery, 2003).

Together, these findings suggest a feeding circuit in which *daf-7* signaling from ASI sensory neurons acts on RIM and RIC interneurons to inhibit tyraminergic and octopaminergic neurotransmissions from these interneurons. When adverse environmental conditions inactivate *daf-7*, its inhibitory effects on tyramine and octopamine are relieved, and in turn, tyraminergic signaling reduces feeding rate largely via signaling to the SER-2 receptor on a small subset of pharyngeal neurons that regulate activity of the pharyngeal muscle.

daf-7 Regulation of Feeding Is Distinct From Fat Accumulation and Dauer Formation

Elimination of tyraminergic and octopaminergic signaling by each of *tdc-1*, *tbh-1*, and *ser-2* mutations restored nearly wild-type feeding rate to *daf-1(−)* animals without altering larval constitutive dauer formation, adult egg retention and excess fat phenotypes of this mutant. This was reminiscent of the finding that inactivation of the *daf-12* abrogated the dauer constitutive but not the fat, feeding, and egg retention phenotypes caused by *daf-7* inactivation. Accordingly, *daf-1(−); tdc-1(−); daf-12(−)* and *daf-1(−); tbh-1(−); daf-12(−)* triple mutants bypassed dauer entry and, as adults, displayed nearly wild-type feeding rates yet accumulated excess fat and retained eggs (Figure 4B–C and data not shown). Together, these findings suggested that, upon DAF-3 activation in RIM and RIC, distinct molecular pathways are engaged to regulate food intake behavior, growth, and metabolism: the effects on growth are eventually mediated by the DAF-12 nuclear hormone receptor while the effects on feeding behavior are mediated by RIM/RIC synthesized neurotransmitters, tyramine and octopamine.

daf-7 Inactivation Causes Fat Accumulation through GPCR Signaling

The FOXO transcription factor encoded by *daf-16* is required for the excess fat, long lifespan, stress resistance, and dauer constitutive phenotypes associated with inhibition of *C. elegans* insulin signaling (Lin et al., 1997; Ogg et al., 1997). However, dauer constitutive or excess fat phenotypes of *daf-7* mutants were independent of this insulin-signaling regulated transcription factor (Ogg et al., 1997).

To identify mechanisms that underlie excess fat accumulation of *daf-7* mutants, we conducted a mutagenesis screen. If the fat, feeding, and dauer responses elicited by *daf-7* inactivation are mediated through distinct mechanisms, we asked whether we could identify mutations that specifically abrogate *daf-1(−)* fat increase without concomitant abrogation of other phenotypes of this mutant. Among several such mutants identified, one line, *daf-1(m40 ft9)*, was selected for further analysis. When dauer constitutive *daf-1(m40 ft9)* mutants were allowed to bypass the dauer stage, they grew to adults that had wild-type fat levels (Figure S4A), were hyperactive, egg laying constitutive and displayed loopy movement and vulval protrusion (data not shown). Similar results were obtained for *daf-7(e1372 ft9)* mutants. The *ft9* suppressor was mapped to *egl-30* (Figure S4 data not shown), which encodes a G_q class α subunit of heterotimeric G proteins (Bastiani et al., 2003; Schade et al., 2005). The G to T nucleotide base change in *egl-30* sequence obtained from *daf-7(e1372); egl-30(ft9*) but absent in wild-type or *daf-7(e1372)* is predicted to result in a glutamic to aspartic acid substitution in a highly

conserved residue within a phylogenetically conserved domain (Figure S4B–D). The semi-dominant segregation as well as movement and egg-laying phenotypes of *egl-30(ft9)* are consistent with previously described *egl-30* gain-of-function (*gof)* mutations (Bastiani et al., 2003; Schade et al., 2005).

EGL-30/$G_q\alpha$ signaling through phospholipase C-β generates the second messenger diacylglycerol while $G_0\alpha$ signaling inhibits its accumulation through activity of DGK-1 kinase (Miller et al., 1999). Thus, phenotypes caused by gain of function mutations in *egl-30* can be mimicked by loss of function mutations in *goa-1* and *dgk-1* (Hajdu-Cronin et al., 1999; Miller et al., 1999; Segalat et al., 1995). *goa-1(−)* or *dgk-1(−)* did not significantly alter fat levels of wild-type animals but reduced the excess fat of *daf-7(−)* mutants to nearly wild-type levels (Figure 5B–C and data not shown). *daf-7(−); egl-30(gof)* as well as *daf-7(−); goa-1(−)*, and *daf-7(−); dgk-1(−)* double mutants remained dauer constitutive and, as adults, displayed reduced feeding rates (Figure 5A and data not shown). While these findings supported the notion that fat and feeding could be regulated through distinct signaling pathways, interpretation of the results were confounded by the fact that numerous processes including pharyngeal pumping, egg laying, and movement involve G-protein signaling.

daf-7 Inactivation Causes Excess Fat Via Metabotropic Glutamate Signaling

To identify signals that may be specifically required for excess fat in *daf-7(−)*, we analyzed neurotransmitter and neuropeptide pathways that utilize GPCR signaling. The *C. elegans* genome encodes ~250 predicted neuropeptides, a subset of which are processed by the subtilisin-family proprotein convertase EGL-3 (Husson et al., 2006). Wild-type processing of at least 25% of predicted neuropeptides is altered in *egl-3* mutants, one consequence of which is reduced fat content (Husson et al., 2007). However, EGL-3 activity was dispensable for excess fat of *daf-7(−)* (data not shown). Similarly, mutations in *unc-17* (Alfonso et al., 1993) and *cat-2* (Lints and Emmons, 1999) which abrogate acetylcholine and dopamine signaling pathways, respectively, did not alter fat accumulation in *daf-7* mutants (data not shown). By contrast, inactivation of the vesicular glutamate transporter encoded by *eat-4* (Lee et al., 1999) partially abrogated excess fat of *daf-7(−)* without suppressing the reduced feeding or dauer constitutive phenotypes of this mutant (Figure 5A–C and data now shown). Unambiguous dissociation of fat and feeding regulation was again confounded since glutamate signaling also regulates feeding rate (Avery, 1993b; Lee et al., 1999).

Given requirements of GPCR and glutamate pathways, we tested whether metabotropic glutamate signaling promotes fat accumulation upon *daf-7* inhibition. The *C. elegans* genome encodes for three metabotropic glutamate receptors, *mgl-1*, *-2*, and *-3* (Dillon et al., 2006). Loss of either *mgl-1* or *mgl-3* but not *mgl-2* reduced the excess fat of *daf-7* mutants from ~245% to ~170% of wild-type levels ($p<0.001$) (Figures 5C and S5). Combination of *mgl-1(−)* and *mgl-3 (−)* further reduced excess fat accumulation of *daf-7* mutants to ~135% of wild-type levels (Figure 5B–C). Despite nearly normalized fat levels, these triple mutants remained dauer constitutive, retained eggs, and displayed reduced feeding rates that were indistinguishable from *daf-7(−)* (Figure 5A, Table S1 and data not shown). Importantly, *mgl-1(−)* and *mgl-3 (−)* mutants had wild-type feeding rates allowing for unambiguous dissociation of fat and feeding mechanisms elicited by *daf-7* inactivation (Figure 5A, Table S1). Finally, to investigate the specificity of metabotropic glutamate receptors in suppressing excess fat levels of *daf-7 (−)* mutants, we investigated the consequences of inactivation in *nmr-1* and *glr-1*, which encode for an N-methyl-D-aspartate (NMDA) and a non-NMDA class of ionotropic glutamate receptors, respectively (Brockie et al., 2001; Hart et al., 1995). *nmr-1(−)* and *glr-1(−)* mutants had wild-type fat accumulation and did not alter the excess fat of *daf-7(−)* (data not shown). This supported the notion that the excess fat of *daf-7(−)* is dependent on activation of specific glutamergic receptors.

To determine potential sites of *mgl-1 and mgl-3* function, we generated reporter fusions to each of their predicted promoters. These promoter fusions were expressed in a very limited number of neurons and only overlapped in the serotonergic pharyngeal NSM neurons (Figure 5D). The largely non-overlapping expression patterns of these reporter fusions were consistent with redundant functions of *mgl-1* and *mgl-3* in mediating excess fat of *daf-7* mutants.

daf-7 mutants have increased *de novo* fat synthesis

Given that excess fat accumulation in *daf-7* and *daf-1* mutants could not be attributed to molecular mechanisms mediating the consequences of inactivation of this pathway on feeding, egg laying and growth, we sought to determine the effects of *daf-7(−)* on metabolic pathways. As an initial characterization, we examined *de novo* rates of fat synthesis. By following the incorporation of 13C labeled carbons into palmitate, stearate, and vaccenic acids extracted from *C. elegans* lysates, we obtained estimates for the fraction of total lipids that were synthesized *de novo*. Relative to wild type, fat synthesis was upregulated nearly ~3 fold in *daf-7* and *daf-1* mutants and this upregulation was dependent on *daf-3* (Figure S6A and data not shown).

To further investigate the role of *de novo* fat synthesis in excess fat of *daf-7* and *daf-1* mutants, we used RNAi to inactivate *fasn-1*, encoding fatty acid synthase. Fatty acid synthase carries out the cyclical reactions that generate fats from malonyl-CoA (Asturias et al., 2005). Exposure of wild-type, *daf-7(−)* and *daf-1(−)* animals to *fasn-1* RNAi resulted in larval growth arrest (example in Figure S6B). Growth arrested *daf-7* and *daf-1* mutants had reduced fat levels indistinguishable from growth arrested wild-type animals (Figure S6B-C and data not shown). Finally, we determined that a ~6kb predicted *fasn-1* promoter-reporter fusion was expressed in epidermal skin-like tissue (hypodermis) (Figure S6D). Epidermal expression is consistent with the metabolic role of *fasn-1* since epidermal and intestinal cells are major sites of fat storage and metabolism in *C. elegans* (Kimura et al., 1997; Mak et al., 2006; McKay et al., 2003). Together, these results indicate that *fasn-1* is critical for fat synthesis and growth and that inactivation of *daf-7* initiates a signaling cascade that ultimately promotes *de novo* fat synthesis in the periphery providing one explanation for the excess fat despite reduced feeding rate.

Discussion

Independent Neural Signaling Pathways Regulate Fat and Feeding

We delineated a genetic and corresponding neuronal circuit that links an environmental sensory mechanism to the regulation of fat content and food intake behavior in *C. elegans*. Adverse environmental conditions such as increased population density and low food availability inactivate the neurally expressed DAF-7 TGF-β like ligand leading to reduced feeding rate, retention of eggs, and shift of energetic resources into fat reservoirs. Inhibition of *daf-7* elicits these responses even in the presence of plentiful food and uncrowded conditions suggesting that perception of unfavorable conditions promotes fat storage. Since *daf-7* is exclusively expressed in the ASI neurons and these neurons have been implicated in the regulation of lifespan by dietary restriction (Bishop and Guarente, 2007), it is possible that, as a gauge of conditions, *daf-7* may be subject to regulation by both external and internal cues of nutrient status.

Our analyses provide a solution to the paradoxical increase in fat despite reduced feeding rate by revealing that *daf-7* regulation of fat is molecularly independent from *daf-7* regulation of feeding. This molecular divergence abrogates the requirement of increased feeding rate as the sole basis of increased fat accumulation. Excess fat accumulation in *daf-7* mutants is associated with increased rate of *de novo* fat synthesis in peripheral tissues. Therefore, while the rate of

food intake is reduced, energetic resources are preferentially directed into build up of fat reservoirs, an adaptive response in preparation for periods of nutrient deprivation (Wang et al., 2006).

The combination of tissue specific expression studies, pharmacology, and genetic epistasis analyses presented here strongly support a model whereby under favorable environmental conditions, DAF-7 signaling from the ASI sensory neurons to its receptors on RIM and RIC interneurons inhibits DAF-3 activation allowing for wild-type fat content, feeding rate and reproduction. Under poor environmental conditions, DAF-3 activation in RIM and RIC leads to tyraminergic regulation of feeding via the SER-2 receptor on pharyngeal neurons and glutamatergic regulation of fat through MGL-1 and MGL-3 metabotropic receptors (Figure 6). Since *mgl-1* and *mgl-3* reporter fusions localize to only a few neurons, activation of metabotropic glutamate signaling in these neurons must initiate other neural or hormonal signals that ultimately signal to sites of fat regulation to shift the balance between storage and utilization pathways.

RIM/RIC activation of DAF-3 also regulates the decision for larval stage animals to grow reproductively or enter hibernation. Genetic and biochemical analyses have placed the DAF-9 cytochrome P450 enzyme downstream of *daf-3* and upstream of the *daf-12* nuclear hormone receptor in the dauer entry pathway (Albert and Riddle, 1988; Gerisch and Antebi, 2004; Gerisch et al., 2001; Jia et al., 2002; Thomas et al., 1993). DAF-9 synthesizes steroid hormone ligands that bind to DAF-12 to inhibit dauer formation and induce reproductive growth (Motola et al., 2006). *daf-9* is expressed in epidermal cells, the pair XXX head cells that are associated with the epidermis, and hermaphrodite spermathecae (Gerisch and Antebi, 2004; Mak and Ruvkun, 2004). Selective reconstitution of *daf-9* in epidermal cells is sufficient to rescue the dauer constitutive but not the egg-laying defect of *daf-7(−)* (Gerisch and Antebi, 2004; Mak and Ruvkun, 2004). Combining these findings with our results, we speculate that signaling from RIM/RIC to epidermal cells regulates DAF-9 during the dauer entry program. Epidermal expressions of *fasn-1* and *daf-9* suggest that this tissue is a major peripheral recipient of neural signals that alter fat and sterol pathways in *C. elegans*.

The only signals that unambiguously originate in RIM and RIC are tyramine and octopamine. Thus, it is possible that an as of yet unidentified signal originates in RIM and RIC that commonly regulates fat, dauer, and egg retention. Upon release from RIM and RIC, this signal must then diverge into glutamergic regulation of fat and other molecular pathways that regulate egg retention and dauer formation (Figure 6).

Neuronal Circuitry of Energy Balance

Why should behavioral, physiological, and metabolic responses regulated by *daf-7* signaling be funneled through very specific pairs of interneurons and subsequently diverge into distinct molecular pathways? As interneurons, RIM and RIC are recipients of multiple neural inputs (White et al., 1986). This allows for integration of various cues regarding energy availability and demand. In turn, regulation of diverse behavioral, physiological, and metabolic responses through distinct molecular outputs allows for fine-tuning and even short-circuiting of individual outputs. Such a differential regulation may be required under different enviromental conditions. For instance, food sources that range in their nutrient qualities or presence of conflicting environmental cues could require differential activation of food-related responses. The *daf-7* circuitry described here provides an efficient solution for simultaneously allowing for coordination while maintaining the flexibility for differential modulation of responses.

The *daf-7* circuit from ASI sensory neurons to RIM and RIC interneurons would not be predicted from the *C. elegans* neural wiring diagram since there are no direct synaptic connections from ASI onto RIM or RIC. Both *C. elegans* and mammalian neurons secrete a

large number of peptides associated with profound behavioral and physiological effects (Ludwig and Leng, 2006). Since peptidergic circuits are not confined by synaptic connections, elucidation of such circuits poses a major challenge that is particularly relevant to mammalian hypothalamus as it is enriched in neurons that secrete a plethora of peptides (Seeley and Woods, 2003).

Conserved Mechanisms of Energy Balance in *C. elegans* and Mammals

Since energy balance is fundamental to organismal survival, we speculate that the basic organizational logic as well as molecular components of energy balance identified in *C. elegans* are likely conserved in mammals. Given identification of metabotropic glutamate signaling in neural regulation of fat in *C. elegans*, it is intriguing that adult mice mutant in metabotropic glutamate receptor subtype 5 weigh significantly less than controls while having a similar ad libitum food intake (Bradbury et al., 2005). Furthermore, we identified tyramine, functional counterpart of vertebrate noradrenaline (Roeder, 2005), as a modulator of *C. elegans* feeding. Insertion of crystalline noradrenaline in the lateral hypothalamus enhances feeding while pharmacological inhibition of its synthesis decreases meal size in satiated rats (Ramos et al., 2005). Thus, excess noradrenaline signaling mimics perception of hunger just as *C. elegans* tyramine signaling elicits a food intake behavior normally caused by food deprivation. Moreover, genetic dissection of mammalian energy regulatory neurocircuits already point to functional and anatomical divergence of brain areas that independently regulate feeding behavior and energy expenditure. For instance, inactivation of melanocortin-4-receptor (MC4R) causes severe obesity marked by hyperphagia and reduced energy expenditure in rodents and humans (Huszar et al., 1997; Vaisse et al., 1998). By genetically reactivating MC4R expression in subsets of rodent neurons, Balthasar and colleagues showed that functional reconstitution of MC4R in the paraventricular nucleus of the hypothalamus and amygdala fully corrects the hyperphagia of MC4R null mice (Balthasar et al., 2005). These mice still develop obesity because of reduced energy expenditure suggesting that MC4R regulates feeding and energy expenditure through distinct neural sites (Balthasar et al., 2005).

In summary, we functionally characterized a *C. elegans* molecular and neural circuit that regulates fat and feeding in response to sensory cues. Rather than feeding as the primary determinant of fat regulation, we found that these pathways are coordinated but independent outputs of the nervous system. Aberrant activation of neural fat promoting pathways can therefore lead to excess fat accumulation without concomitant increases in feeding rate.

Experimental Procedures

C. elegans Maintenance and Strain Constructions

Nematodes were grown and maintained on NGM plates using OP50 *E. coli* bacteria as food source as described (Brenner, 1974). Dauer constitutive strains were maintained at the permissive temperature of 20°C. Although *daf-1(m40)* and *daf-7(e1372)* dauer phenotypes are temperature sensitive, neither the pumping rate nor the fat phenotypes depended on temperature.

Strains were obtained from the CGC (www.cbs.umn.edu/CGC/), OMRF Knockout Consortium (www.mutantfactory.ouhsc.edu/), and the National Bio-resources Project (shigen.lab.nig.ac.jp/c.elegans/) (Table S1). When generating double and triple mutants (Table S1), animals with desired combination of mutations were confirmed by PCR and sequencing.

Sudan Black Fat Staining and Quantitation

All Sudan black assays were performed at room temperature (22°C) as previously described (Kimura et al., 1997) with the following modification to minimize staining variability which

allowed for quantitative comparisons between various genotypes: animals from one genotype were labeled with FITC and then fixed and stained in the same tube as unlabeled animals from another genotype. For transgenic lines, fat phenotype was assayed by comparing transgenic animals marked with $P_{odr\text{-}1}$*::dsRED* and non-transgenic animals, which were fixed and stained in the same tube. Genotype combinations that caused a significant change in Sudan black stainings of *daf-7(e1372)* or *daf-1(m40)* were tested at least 5 independent times giving consistent results. Genotype combinations that did not significantly alter the excess fat of *daf-7 (e1372)* or *daf-1(m40)* strains were tested in at least two independent experiments. For quantitation, Sudan black images were collected on a Zeiss Axioplan 2 microscope fitted with a Hamamatsu Orca-AG camera. Staining intensities were quantitated using Improvision Openlab software. Mean pixel intensity was calculated for staining in the region from the first intestinal cells adjacent to the pharynx midway through the animal to the vulva. Background was determined based on pixel intensity of nonspecific staining in the pharynx. Values are reported as mean pixel intensity minus background for at least ten randomly selected test and control animals fixed and stained in the same tube.

Pharyngeal Pumping Assay

Well-fed condition: synchronized L1 stage larvae were grown on OP50 *E. coli* at low density at 20°C. Pharyngeal pumping rate was counted at room temperature for individual well-fed, gravid adults using a Zeiss M^2 BIO microscope and an electronic counter (Diffcount). Number of pumps of individual animals was counted in 15-second intervals. Normally, pumping rates of ~20 animals were counted per genotype per day. These counts were repeated on at least 3 independent assays performed on separate days.

Food deprived condition: well-fed young animals were washed off plates and rinsed twice with S-basal buffer (Brenner, 1974) and maintained in S-basal in a rotating 15ml conical tube for 30 minutes. Animals were then spun into a pellet, rinsed, and plated on unseeded plates. Pumping rates were measured for ~20 animals per genotype 30 minutes post plating. These counts were repeated at least 3 independent times.

Dauer pheromone treatment: 30 animals grown to the desired stages (late larval stage/young adult) under well-fed conditions were transferred to pheromone plates containing 30 μl/ml of a dauer pheromone prep (Golden and Riddle, 1982) and 30 μl of OP50 *E. coli* food. These conditions caused dauer entry in ~75% of early larval stage animals. The reported values are averages of 20 animals per genotype per assay. Assays were repeated three independent times.

Dauer and Egg-retention Assays

Synchronized L1 animals were seeded at low density on plates with plentiful *OP50 E. coli* at 25°C. The plates were maintained at 25°C and numbers of adults and dauer larvae were counted three days after plating. Dauers were identified based on their dramatic visual characteristics (example in Figure S1). To confirm this visual inspection, in select cases, animals were washed off plates and subjected to 1% SDS treatment and surviving animals were counted (Cassada and Russell, 1975). To assess egg retention phenotype, animals were synchronized and grown under well-fed conditions at low density. Egg retention was scored in 2-day-old adults.

Plasmid and GFP-Reporter Fusion Constructs

Plasmids for tissue reconstitution rescue lines were constructed using Gateway Technology (www.invitrogen.com). The *daf-1* ORF was obtained from the *C. elegans* ORFeome (www.openbiosystems.org). The *daf-3* genomic DNA was cloned using *C. elegans* ORFeome primers and the pDONR-221 vector (Deplancke et al., 2004; Dupuy et al., 2004). Promoters for *egl-3, bbs-1, osm-6, glr-8, B0280.7, glr-1, glr-5, unc-17, glr-2, glr-4, unc-47, ggr-2, flp-1, dop-1, nmr-2, myo-2 and flp-18* were constructed using Promoterome primers and the pDONR-

P4-P1R vector (Deplancke et al., 2004; Dupuy et al., 2004). These promoters generally contained 2 kb of genomic sequence upstream of the corresponding gene's ATG start site. Promoters for *daf-1, daf-7, glr-7, tbh-1, tdc-1,* and *hsp16.2* were generated using primers to amplify published promoter lengths (Alkema et al., 2005; Brockie et al., 2001a; Gunther et al., 2000; Ren et al., 1996). Rescue constructs were generated using the pDEST-MB14 (*daf-1* and *daf-1;daf-3* rescue) or modified plasmid pKA453 (*daf-1;ser-2* rescue) which lacks the *unc-119* rescue region and contains a polycistronic GFP fusion. Rescue constructs were generated using the pDEST-MB14 plasmid to obtain *promoter::daf-1-ORF::gfp* or *promoter::daf-3::gfp* translational fusions (Vaglio et al., 2003) such that *gfp* was fused in frame to the C-terminal end of *daf-1* ORF where the *daf-1* stop codon had been eliminated. Expression patterns of these translational full-length fusions were compared to expression patterns of *promoter::gfp* transcriptional fusions constructed by using pDEST-DD04 vector.

Transgenic Animals

For tissue-specific rescue experiments, *daf-1(m40), daf-1(m40); daf-3(mgDf90),* and *daf-1 (m40); ser-2(pk1357)* animals were injected with plasmid of interest at a concentration of 20ng/μl and co-injection marker $P_{odr\text{-}1}$*::dsRED* at a concentration of 30ng/μl. At least three independent lines were generated for each transgene.

Heat Shock Activation of $P_{hsp16.2}$*::daf-1* Transgene

Synchronized L1 stage control and test animals were grown to L3/L4 or the adult stage at 20° C, then subjected to 34°C heat shock for 45 minutes. Heat shocked animals were allowed to recover at room temperature for 1 hr. Fat, feeding, and egg retention phenotypes were assayed 30 minutes to 24 hrs post recovery.

Genetic Screening and Molecular Mapping

~2500 *daf-1(m40)* animals were EMS mutagenized (Brenner, 1974). ~24,000 resulting F_1 progeny were grown at 20°C and equally divided into 15 pools. These pools were allowed to self fertilize giving rise to ~125,000 F_2 progeny. These animals were visually inspected for dark intestine, egg retention, and Nile Red staining at 20°C (Ashrafi et al. 2003). Hermaphrodites with the desired phenotypes were singled onto plates and allowed to reproduce. F_1 progeny of these hermaphrodites were then re-examined for the desired phenotypes and F_2 progeny were divided into two groups, one of which was examined for constitutive dauer entry at 26.5°C and the other was assayed for Sudan black staining.

The *ft9* suppressor was crossed into *daf-7(e1372)* animals and backcrossed four times. For mapping purposes, we generated a CB4856 strain carrying the Bristol *daf-7(e1372)* locus. The *ft9* suppressor was mapped using standard single nucleotide polymorphism techniques (Jakubowski and Kornfeld, 1999).

Biochemical Assessment of Fat Synthesis

Synchronized *C. elegans* were grown on a mixture of unlabeled bacteria and 13C labeled bacteria. Total lipid was purified, converted to fatty acid methyl esters and analyzed by GC/MS (Watts and Browse, 2002). The fraction of palmitic, stearic, and vaccenic fatty acid produced via *de novo* fatty acid synthesis, as opposed to fatty acid obtained from direct dietary absorption, was calculated based on the relative isotope distribution.

Anatomical Methods

Identities of cells expressing gene-reporter fusions were determined by standard anatomical methods including dye filling of amphid neurons to help orient positions of various neurons.

Supplementary Material

Refer to Web version on PubMed Central for supplementary material.

Acknowledgements

E.R.G was supported by a predoctoral fellowship from the American Heart Association. This work was supported by an RO1 grant from the NIH/NIDDK (DK070149), The Sandler Family Fund, The Searle Scholars Program and The Burroughs Wellcome Fund. We thank the Bargmann and Vidal labs for plasmids. We are grateful to members of the Ashrafi lab, Henry Bourne, Holly Ingraham, Roland Bainton, and Nils Faergeman for discussions and suggestions.

References

Albert PS, Riddle DL. Mutants of Caenorhabditis elegans that form dauer-like larvae. Dev Biol 1988;126:270–293. [PubMed: 3350212]

Alfonso A, Grundahl K, Duerr JS, Han HP, Rand JB. The Caenorhabditis elegans unc-17 gene: a putative vesicular acetylcholine transporter. Science 1993;261:617–619. [PubMed: 8342028]

Alkema MJ, Hunter-Ensor M, Ringstad N, Horvitz HR. Tyramine Functions independently of octopamine in the Caenorhabditis elegans nervous system. Neuron 2005;46:247–260. [PubMed: 15848803]

Ansley SJ, Badano JL, Blacque OE, Hill J, Hoskins BE, Leitch CC, Kim JC, Ross AJ, Eichers ER, Teslovich TM, Mah AK, Johnsen RC, Cavender JC, Lewis RA, Leroux MR, Beales PL, Katsanis N. Basal body dysfunction is a likely cause of pleiotropic Bardet-Biedl syndrome. Nature 2003;425:628–633. [PubMed: 14520415]

Antebi A, Yeh WH, Tait D, Hedgecock EM, Riddle DL. daf-12 encodes a nuclear receptor that regulates the dauer diapause and developmental age in C. elegans. Genes Dev 2000;14:1512–1527. [PubMed: 10859169]

Ashrafi K, Chang FY, Watts JL, Fraser AG, Kamath RS, Ahringer J, Ruvkun G. Genome-wide RNAi analysis of Caenorhabditis elegans fat regulatory genes. Nature 2003;421:268–272. [PubMed: 12529643]

Asturias FJ, Chadick JZ, Cheung IK, Stark H, Witkowski A, Joshi AK, Smith S. Structure and molecular organization of mammalian fatty acid synthase. Nat Struct Mol Biol 2005;12:225–232. [PubMed: 15711565]

Avery L. Motor neuron M3 controls pharyngeal muscle relaxation timing in Caenorhabditis elegans. J Exp Biol 1993a;175:283–297. [PubMed: 8440973]

Avery L. The genetics of feeding in Caenorhabditis elegans. Genetics 1993b;133:897–917. [PubMed: 8462849]

Avery L, Horvitz HR. Pharyngeal pumping continues after laser killing of the pharyngeal nervous system of C. elegans. Neuron 1989;3:473–485. [PubMed: 2642006]

Avery L, Horvitz HR. Effects of starvation and neuroactive drugs on feeding in Caenorhabditis elegans. J Exp Zool 1990;253:263–270. [PubMed: 2181052]

Bacaj T, Shaham S. Temporal control of cell-specific transgene expression in Caenorhabditis elegans. Genetics 2007;176:2651–2655. [PubMed: 17603102]

Balthasar N, Coppari R, McMinn J, Liu SM, Lee CE, Tang V, Kenny CD, McGovern RA, Chua SC Jr, Elmquist JK, Lowell BB. Leptin receptor signaling in POMC neurons is required for normal body weight homeostasis. Neuron 2004;42:983–991. [PubMed: 15207242]

Balthasar N, Dalgaard LT, Lee CE, Yu J, Funahashi H, Williams T, Ferreira M, Tang V, McGovern RA, Kenny CD, Christiansen LM, Edelstein E, Choi B, Boss O, Aschkenasi C, Zhang CY, Mountjoy K, Kishi T, Elmquist JK, Lowell BB. Divergence of melanocortin pathways in the control of food intake and energy expenditure. Cell 2005;123:493–505. [PubMed: 16269339]

Bastiani CA, Gharib S, Simon MI, Sternberg PW. Caenorhabditis elegans Galphaq regulates egg-laying behavior via a PLC beta-independent and serotonin-dependent signaling pathway and likely functions both in the nervous system and in muscle. Genetics 2003;165:1805–1822. [PubMed: 14704167]

Bishop NA, Guarente L. Two neurons mediate diet-restriction-induced longevity in C. elegans. Nature 2007;447:545–549. [PubMed: 17538612]

Bradbury MJ, Campbell U, Giracello D, Chapman D, King C, Tehrani L, Cosford ND, Anderson J, Varney MA, Strack AM. Metabotropic glutamate receptor mGlu5 is a mediator of appetite and energy balance in rats and mice. J Pharmacol Exp Ther 2005;313:395–402. [PubMed: 15590770]

Brenner S. The genetics of Caenorhabditis elegans. Genetics 1974;77:71–94. [PubMed: 4366476]

Brock TJ, Browse J, Watts JL. Fatty acid desaturation and the regulation of adiposity in Caenorhabditis elegans. Genetics 2007;176:865–875. [PubMed: 17435249]

Brockie PJ, Madsen DM, Zheng Y, Mellem J, Maricq AV. Differential expression of glutamate receptor subunits in the nervous system of Caenorhabditis elegans and their regulation by the homeodomain protein UNC-42. J Neurosci 2001a;21:1510–1522. [PubMed: 11222641]

Brockie PJ, Mellem JE, Hills T, Madsen DM, Maricq AV. The C. elegans glutamate receptor subunit NMR-1 is required for slow NMDA-activated currents that regulate reversal frequency during locomotion. Neuron 2001b;31:617–630. [PubMed: 11545720]

Butcher RA, Fujita M, Schroeder FC, Clardy J. Small-molecule pheromones that control dauer development in Caenorhabditis elegans. Nat Chem Biol 2007;3:420–422. [PubMed: 17558398]

Cassada RC, Russell RL. The dauer larva, a post-embryonic developmental variant of the nematode Caenorhabditis elegans. Dev Biol 1975;46:326–342. [PubMed: 1183723]

Collet J, Spike CA, Lundquist EA, Shaw JE, Herman RK. Analysis of osm-6, a gene that affects sensory cilium structure and sensory neuron function in Caenorhabditis elegans. Genetics 1998;148:187–200. [PubMed: 9475731]

de Luca C, Kowalski TJ, Zhang Y, Elmquist JK, Lee C, Kilimann MW, Ludwig T, Liu SM, Chua SC Jr. Complete rescue of obesity, diabetes, and infertility in db/db mice by neuron-specific LEPR-B transgenes. J Clin Invest 2005;115:3484–3493. [PubMed: 16284652]

Deplancke B, Dupuy D, Vidal M, Walhout AJ. A gateway-compatible yeast one-hybrid system. Genome Res 2004;14:2093–2101. [PubMed: 15489331]

Dhillon H, Zigman JM, Ye C, Lee CE, McGovern RA, Tang V, Kenny CD, Christiansen LM, White RD, Edelstein EA, Coppari R, Balthasar N, Cowley MA, Chua S Jr, Elmquist JK, Lowell BB. Leptin directly activates SF1 neurons in the VMH, and this action by leptin is required for normal body-weight homeostasis. Neuron 2006;49:191–203. [PubMed: 16423694]

Dillon J, Hopper NA, Holden-Dye L, O'Connor V. Molecular characterization of the metabotropic glutamate receptor family in Caenorhabditis elegans. Biochem Soc Trans 2006;34:942–948. [PubMed: 17052233]

Douglas SJ, Dawson-Scully K, Sokolowski MB. The neurogenetics and evolution of food-related behaviour. Trends Neurosci 2005;28:644–652. [PubMed: 16203044]

Dupuy D, Li QR, Deplancke B, Boxem M, Hao T, Lamesch P, Sequerra R, Bosak S, Doucette-Stamm L, Hope IA, Hill DE, Walhout AJ, Vidal M. A first version of the Caenorhabditis elegans Promoterome. Genome Res 2004;14:2169–2175. [PubMed: 15489340]

Eastman C, Horvitz HR, Jin Y. Coordinated transcriptional regulation of the unc-25 glutamic acid decarboxylase and the unc-47 GABA vesicular transporter by the Caenorhabditis elegans UNC-30 homeodomain protein. J Neurosci 1999;19:6225–6234. [PubMed: 10414952]

Elmquist JK, Maratos-Flier E, Saper CB, Flier JS. Unraveling the central nervous system pathways underlying responses to leptin. Nat Neurosci 1998;1:445–450. [PubMed: 10196541]

Estevez M, Attisano L, Wrana JL, Albert PS, Massague J, Riddle DL. The daf-4 gene encodes a bone morphogenetic protein receptor controlling C. elegans dauer larva development. Nature 1993;365:644–649. [PubMed: 8413626]

Fulton S, Pissios P, Manchon RP, Stiles L, Frank L, Pothos EN, Maratos-Flier E, Flier JS. Leptin regulation of the mesoaccumbens dopamine pathway. Neuron 2006;51:811–822. [PubMed: 16982425]

Georgi LL, Albert PS, Riddle DL. daf-1, a C. elegans gene controlling dauer larva development, encodes a novel receptor protein kinase. Cell 1990;61:635–645. [PubMed: 2160853]

Gerisch B, Antebi A. Hormonal signals produced by DAF-9/cytochrome P450 regulate C. elegans dauer diapause in response to environmental cues. Development 2004;131:1765–1776. [PubMed: 15084461]

Gerisch B, Weitzel C, Kober-Eisermann C, Rottiers V, Antebi A. A hormonal signaling pathway influencing C. elegans metabolism, reproductive development, and life span. Dev Cell 2001;1:841–851. [PubMed: 11740945]

Golden JW, Riddle DL. A pheromone influences larval development in the nematode Caenorhabditis elegans. Science 1982;218:578–580. [PubMed: 6896933]

Gunther CV, Georgi LL, Riddle DL. A Caenorhabditis elegans type I TGF beta receptor can function in the absence of type II kinase to promote larval development. Development 2000;127:3337–3347. [PubMed: 10887089]

Hajdu-Cronin YM, Chen WJ, Patikoglou G, Koelle MR, Sternberg PW. Antagonism between G(o)alpha and G(q)alpha in Caenorhabditis elegans: the RGS protein EAT-16 is necessary for G(o)alpha signaling and regulates G(q)alpha activity. Genes Dev 1999;13:1780–1793. [PubMed: 10421631]

Hart AC, Sims S, Kaplan JM. Synaptic code for sensory modalities revealed by C. elegans GLR-1 glutamate receptor. Nature 1995;378:82–85. [PubMed: 7477294]

Hills T, Brockie PJ, Maricq AV. Dopamine and glutamate control area-restricted search behavior in Caenorhabditis elegans. J Neurosci 2004;24:1217–1225. [PubMed: 14762140]

Hommel JD, Trinko R, Sears RM, Georgescu D, Liu ZW, Gao XB, Thurmon JJ, Marinelli M, DiLeone RJ. Leptin receptor signaling in midbrain dopamine neurons regulates feeding. Neuron 2006;51:801–810. [PubMed: 16982424]

Horvitz HR, Chalfie M, Trent C, Sulston JE, Evans PD. Serotonin and octopamine in the nematode Caenorhabditis elegans. Science 1982;216:1012–1014. [PubMed: 6805073]

Husson SJ, Clynen E, Baggerman G, Janssen T, Schoofs L. Defective processing of neuropeptide precursors in Caenorhabditis elegans lacking proprotein convertase 2 (KPC-2/EGL-3): mutant analysis by mass spectrometry. J Neurochem 2006;98:1999–2012. [PubMed: 16945111]

Husson SJ, Janssen T, Baggerman G, Bogert B, Kahn-Kirby AH, Ashrafi K, Schoofs L. Impaired processing of FLP and NLP peptides in carboxypeptidase E (EGL-21)-deficient Caenorhabditis elegans as analyzed by mass spectrometry. J Neurochem 2007;102:246–260. [PubMed: 17564681]

Huszar D, Lynch CA, Fairchild-Huntress V, Dunmore JH, Fang Q, Berkemeier LR, Gu W, Kesterson RA, Boston BA, Cone RD, Smith FJ, Campfield LA, Burn P, Lee F. Targeted disruption of the melanocortin-4 receptor results in obesity in mice. Cell 1997;88:131–141. [PubMed: 9019399]

Jakubowski J, Kornfeld K. A local, high-density, single-nucleotide polymorphism map used to clone Caenorhabditis elegans cdf-1. Genetics 1999;153:743–752. [PubMed: 10511554]

Jeong PY, Jung M, Yim YH, Kim H, Park M, Hong E, Lee W, Kim YH, Kim K, Paik YK. Chemical structure and biological activity of the Caenorhabditis elegans dauer-inducing pheromone. Nature 2005;433:541–545. [PubMed: 15690045]

Jia K, Albert PS, Riddle DL. DAF-9, a cytochrome P450 regulating C. elegans larval development and adult longevity. Development 2002;129:221–231. [PubMed: 11782415]

John D. Annual lipid cycles in hibernators: integration of physiology and behavior. Annu Rev Nutr 2005;25:469–497. [PubMed: 16011475]

Kimura KD, Tissenbaum HA, Liu Y, Ruvkun G. daf-2, an insulin receptor-like gene that regulates longevity and diapause in Caenorhabditis elegans. Science 1997;277:942–946. [PubMed: 9252323]

Krishna S, Maduzia LL, Padgett RW. Specificity of TGFbeta signaling is conferred by distinct type I receptors and their associated SMAD proteins in Caenorhabditis elegans. Development 1999;126:251–260. [PubMed: 9847239]

Lee RY, Sawin ER, Chalfie M, Horvitz HR, Avery L. EAT-4, a homolog of a mammalian sodium-dependent inorganic phosphate cotransporter, is necessary for glutamatergic neurotransmission in caenorhabditis elegans. J Neurosci 1999;19:159–167. [PubMed: 9870947]

Lin K, Dorman JB, Rodan A, Kenyon C. daf-16: An HNF-3/forkhead family member that can function to double the life-span of Caenorhabditis elegans. Science 1997;278:1319–1322. [PubMed: 9360933]

Lints R, Emmons SW. Patterning of dopaminergic neurotransmitter identity among Caenorhabditis elegans ray sensory neurons by a TGFbeta family signaling pathway and a Hox gene. Development 1999;126:5819–5831. [PubMed: 10572056]

Lipton J, Kleemann G, Ghosh R, Lints R, Emmons SW. Mate searching in Caenorhabditis elegans: a genetic model for sex drive in a simple invertebrate. J Neurosci 2004;24:7427–7434. [PubMed: 15329389]

Ludwig M, Leng G. Dendritic peptide release and peptide-dependent behaviours. Nat Rev Neurosci 2006;7:126–136. [PubMed: 16429122]

Mak HY, Nelson LS, Basson M, Johnson CD, Ruvkun G. Polygenic control of Caenorhabditis elegans fat storage. Nat Genet 2006;38:363–368. [PubMed: 16462744]

Mak HY, Ruvkun G. Intercellular signaling of reproductive development by the C. elegans DAF-9 cytochrome P450. Development 2004;131:1777–1786. [PubMed: 15084462]

McKay RM, McKay JP, Avery L, Graff JM. C elegans: a model for exploring the genetics of fat storage. Dev Cell 2003;4:131–142. [PubMed: 12530969]

Miller KG, Emerson MD, Rand JB. Goalpha and diacylglycerol kinase negatively regulate the Gqalpha pathway in C. elegans. Neuron 1999;24:323–333. [PubMed: 10571227]

Morton GJ, Cummings DE, Baskin DG, Barsh GS, Schwartz MW. Central nervous system control of food intake and body weight. Nature 2006;443:289–295. [PubMed: 16988703]

Motola DL, Cummins CL, Rottiers V, Sharma KK, Li T, Li Y, Suino-Powell K, Xu HE, Auchus RJ, Antebi A, Mangelsdorf DJ. Identification of ligands for DAF-12 that govern dauer formation and reproduction in C. elegans. Cell 2006;124:1209–1223. [PubMed: 16529801]

Niacaris T, Avery L. Serotonin regulates repolarization of the C. elegans pharyngeal muscle. J Exp Biol 2003;206:223–231. [PubMed: 12477893]

O'Riordan V, Burnell AM. Intermediary metabolism in the dauer larva of the nematode *C. elegans*. I. Glycolysis gluconeogenesis, oxidative phosphorylation and the tricarboxylic acid cycle. Comp Biochem Physiol 1989;92B:233–238.

Ogg S, Paradis S, Gottlieb S, Patterson GI, Lee L, Tissenbaum HA, Ruvkun G. The Fork head transcription factor DAF-16 transduces insulin-like metabolic and longevity signals in C. elegans. Nature 1997;389:994–999. [PubMed: 9353126]

Okkema PG, Harrison SW, Plunger V, Aryana AAF. Sequence requiremetns for myosin gene expression and regulation in Caenorhabditis elegans. Genetics 1993;135:385–404. [PubMed: 8244003]

Patterson GI, Koweek A, Wong A, Liu Y, Ruvkun G. The DAF-3 Smad protein antagonizes TGF-beta-related receptor signaling in the Caenorhabditis elegans dauer pathway. Genes Dev 1997;11:2679–2690. [PubMed: 9334330]

Ramos EJ, Meguid MM, Campos AC, Coelho JC. Neuropeptide Y, alpha-melanocyte-stimulating hormone, and monoamines in food intake regulation. Nutrition 2005;21:269–279. [PubMed: 15723758]

Ren P, Lim CS, Johnsen R, Albert PS, Pilgrim D, Riddle DL. Control of C. elegans larval development by neuronal expression of a TGF-beta homolog. Science 1996;274:1389–1391. [PubMed: 8910282]

Rex E, Hapiak V, Hobson R, Smith K, Xiao H, Komuniecki R. TYRA-2 (F01E11.5): a Caenorhabditis elegans tyramine receptor expressed in the MC and NSM pharyngeal neurons. J Neurochem 2005;94:181–191. [PubMed: 15953361]

Rex E, Komuniecki RW. Characterization of a tyramine receptor from Caenorhabditis elegans. J Neurochem 2002;82:1352–1359. [PubMed: 12354282]

Rex E, Molitor SC, Hapiak V, Xiao H, Henderson M, Komuniecki R. Tyramine receptor (SER-2) isoforms are involved in the regulation of pharyngeal pumping and foraging behavior in Caenorhabditis elegans. J Neurochem 2004;91:1104–1115. [PubMed: 15569254]

Riddle, DBT.; Meyber, B.; Priess, J. C elegans II. 1997.

Roeder T. Tyramine and octopamine: ruling behavior and metabolism. Annu Rev Entomol 2005;50:447–477. [PubMed: 15355245]

Saper CB, Chou TC, Elmquist JK. The need to feed: homeostatic and hedonic control of eating. Neuron 2002;36:199–211. [PubMed: 12383777]

Sawin ER, Ranganathan R, Horvitz HR. C. elegans locomotory rate is modulated by the environment through a dopaminergic pathway and by experience through a serotonergic pathway. Neuron 2000;26:619–631. [PubMed: 10896158]

Schackwitz WS, Inoue T, Thomas JH. Chemosensory neurons function in parallel to mediate a pheromone response in C. elegans. Neuron 1996;17:719–728. [PubMed: 8893028]

Schade MA, Reynolds NK, Dollins CM, Miller KG. Mutations that rescue the paralysis of Caenorhabditis elegans ric-8 (synembryn) mutants activate the G alpha(s) pathway and define a third major branch of the synaptic signaling network. Genetics 2005;169:631–649. [PubMed: 15489510]

Seeley RJ, Woods SC. Monitoring of stored and available fuel by the CNS: implications for obesity. Nat Rev Neurosci 2003;4:901–909. [PubMed: 14595401]

Segalat L, Elkes DA, Kaplan JM. Modulation of serotonin-controlled behaviors by Go in Caenorhabditis elegans. Science 1995;267:1648–1651. [PubMed: 7886454]

Sternson SM, Shepherd GM, Friedman JM. Topographic mapping of VMH --> arcuate nucleus microcircuits and their reorganization by fasting. Nat Neurosci 2005;8:1356–1363. [PubMed: 16172601]

Stringham EG, Dixon DK, Jones D, Candido EP. Temporal and spatial expression patterns of the small heat shock (hsp16) genes in transgenic Caenorhabditis elegans. Mol Biol Cell 1992;3:221–233. [PubMed: 1550963]

Sze JY, Victor M, Loer C, Shi Y, Ruvkun G. Food and metabolic signalling defects in a Caenorhabditis elegans serotonin-synthesis mutant. Nature 2000;403:560–564. [PubMed: 10676966]

Taubert S, Van Gilst MR, Hansen M, Yamamoto KR. A Mediator subunit, MDT-15, integrates regulation of fatty acid metabolism by NHR-49-dependent and -independent pathways in C. elegans. Genes Dev 2006;20:1137–1149. [PubMed: 16651656]

Thomas JH, Birnby DA, Vowels JJ. Evidence for parallel processing of sensory information controlling dauer formation in Caenorhabditis elegans. Genetics 1993;134:1105–1117. [PubMed: 8375650]

Trent, C. PhD thesis. Cambridge, MA: Massachusetts Institute of Technology; 1982. Genetics and behavioral studies of the egg-laying system of *Canorhabditis elegans*.

Tsalik EL, Niacaris T, Wenick AS, Pau K, Avery L, Hobert O. LIM homeobox gene-dependent expression of biogenic amine receptors in restricted regions of the C. elegans nervous system. Dev Biol 2003;263:81–102. [PubMed: 14568548]

Vaglio P, Lamesch P, Reboul J, Rual JF, Martinez M, Hill D, Vidal M. WorfDB: the Caenorhabditis elegans ORFeome Database. Nucleic Acids Res 2003;31:237–240. [PubMed: 12519990]

Vaisse C, Clement K, Guy-Grand B, Froguel P. A frameshift mutation in human MC4R is associated with a dominant form of obesity. Nat Genet 1998;20:113–114. [PubMed: 9771699]

Van Gilst MR, Hadjivassiliou H, Jolly A, Yamamoto KR. Nuclear hormone receptor NHR-49 controls fat consumption and fatty acid composition in C. elegans. PLoS Biol 2005a;3:e53. [PubMed: 15719061]

Van Gilst MR, Hadjivassiliou H, Yamamoto KR. A Caenorhabditis elegans nutrient response system partially dependent on nuclear receptor NHR-49. Proc Natl Acad Sci U S A 2005b;102:13496–13501. [PubMed: 16157872]

Volkow ND, Wise RA. How can drug addiction help us understand obesity? Nat Neurosci 2005;8:555–560. [PubMed: 15856062]

Wadsworth WG, Riddle DL. Developmental regulation of energy metabolism in Caenorhabditis elegans. Dev Biol 1989;132:167–173. [PubMed: 2917691]

Wang J, Kim SK. Global analysis of dauer gene expression in Caenorhabditis elegans. Development 2003;130:1621–1634. [PubMed: 12620986]

Wang T, Hung CC, Randall DJ. The comparative physiology of food deprivation: from feast to famine. Annu Rev Physiol 2006;68:223–251. [PubMed: 16460272]

Watts JL, Browse J. Genetic dissection of polyunsaturated fatty acid synthesis in Caenorhabditis elegans. Proc Natl Acad Sci U S A 2002;99:5854–5859. [PubMed: 11972048]

White JG, Southgate Thomson E, Brenner JNS. The Structure of the Nervous System of the Nematode *Caenorhabditis Elegans*. Philosophical Transactions of the Royal Society of London 1986;314:1–340.

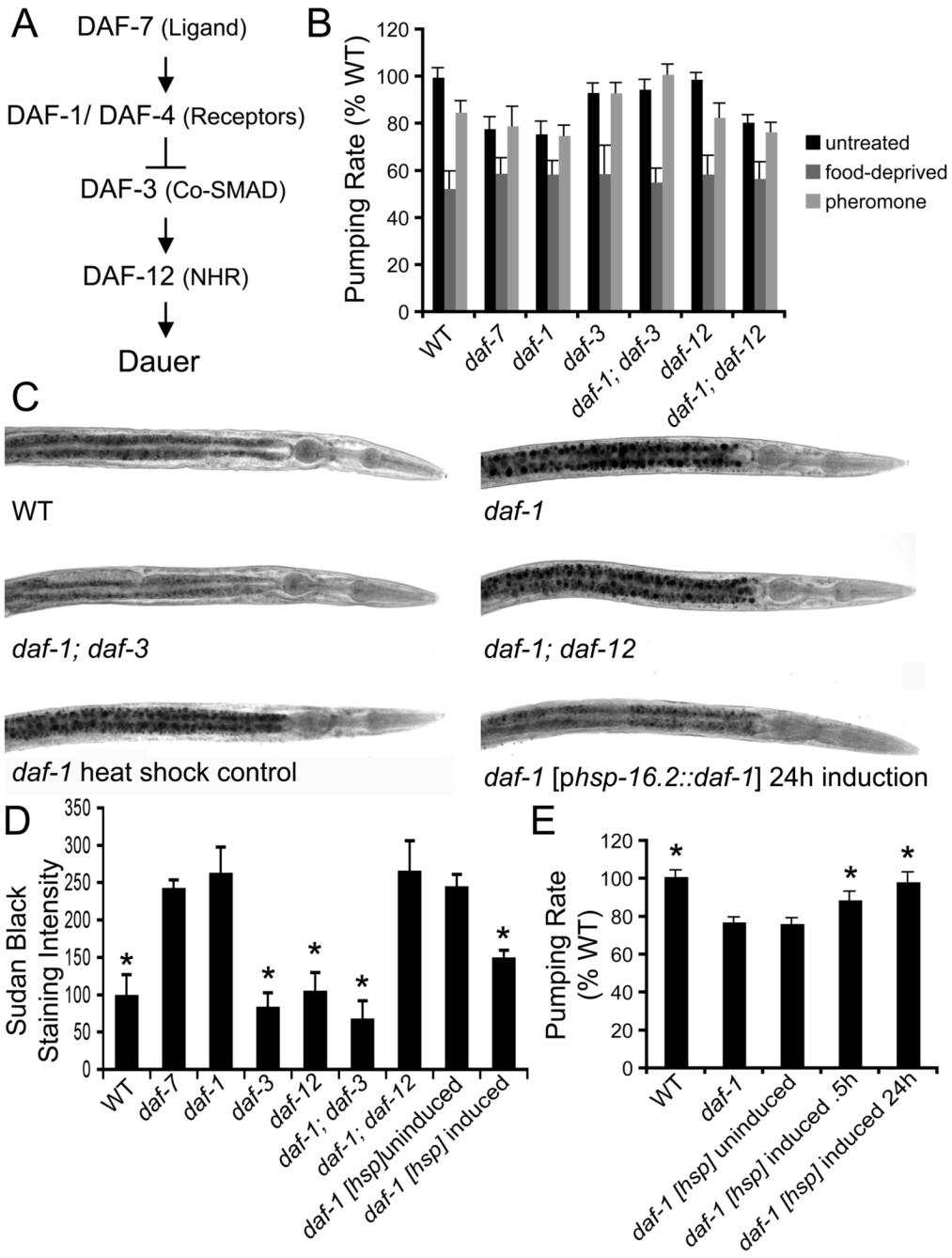

Figure 1. TGF-β Signaling Modulates Feeding Rate and Fat Storage in Adults

(A) TGF-β signaling pathway as deduced from genetic analyses of dauer formation.

(B) Pharyngeal pumping rates of TGF-β pathway components under various conditions. *Well-fed, pheromone untreated: daf-7(e1372)* and *daf-1(m40)* pumped at 81% and 77% of wild-type rate, respectively. The reduced pumping rate of *daf-1(m40)* was suppressed by *daf-3 (mgDf90)* but not by *daf-12(m20). Food deprived, pheromone untreated*: pumping rates of young adult wild type and all mutant genotypes were reduced to the same basal level. *Well-fed, pheromone treated*: treatment caused feeding reduction in well-fed wild type and *daf-12* mutants. Similar treatment did not further reduce feeding rates of *daf-7*, *daf-1*, or *daf-3* mutants. Standard deviation bars are shown.

(C) Examples of Sudan black fat staining. Adult *daf-1(m40)* mutants had increased fat relative to wild type. This excess fat was suppressed by *daf-3(mgDf90)* but not by *daf-12(m20)*. Excess fat of *daf-1(m40)* animals was reduced by expression of *daf-1(+)* in late larval/adult stage animals using an *hsp16.2* heat-shock promoter. These images are representative of numerous animals from each genotype observed in multiple, independent experiments (*see Methods*).
(D) Quantitation of relative amounts of Sudan black staining. Animals grown under identical conditions were fixed and stained using methods designed to minimize variation. For each genotype, average staining intensity of 10 animals is reported. Asterisks indicate statistical significance ($p<0.001$) as determined by t-test when comparing genotype of interest with *daf-1 (m40)*. Standard error bars are shown.
(E) Rescue of reduced pumping rate by expression of *daf-1* in late larval/adult stage *daf-1 (m40)* mutants. Pumping rate changes were noted 0.5h and 24h after induction. Asterisks indicate statistically significant change ($p<0.001$ determined by ANOVA with Bonferroni post-test) relative to *daf-1(m40)*. Standard deviation bars are shown

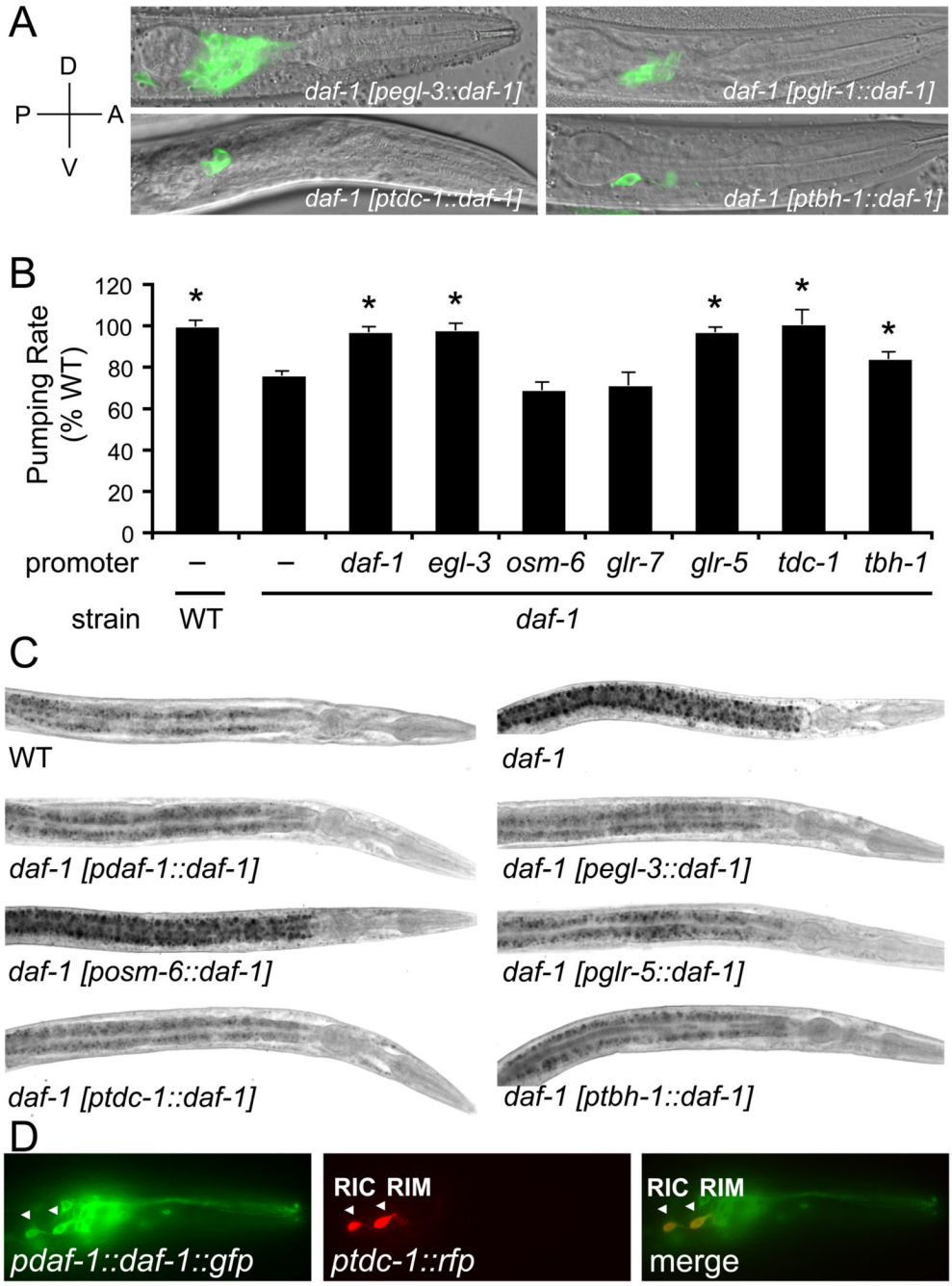

Figure 2. Reconstitution of *daf-1* in RIM and RIC Interneurons Restores Wild-type Feeding Rate and Fat Storage to *daf-1(m40)* Mutants

Tissue-specific promoters listed in Table 1 were used to express full-length *daf-1::gfp* in various cell types of *daf-1(m40)* animals.

(A) Examples of neuronal expression patterns of promoters used to target *daf-1::gfp.* Axis indicates P, posterior, A, anterior, D, dorsal, V, ventral.

(B) Effects of tissue selective reconstitution of *daf-1* on feeding rate. Asterisks indicate statistical significance relative to *daf-1(m40)* ($p<0.001$ as determined by ANOVA with Bonferroni post-test). Standard deviation bars are shown.

(C) Effects of tissue selective reconstitution of *daf-1* on fat. Quantitations for representative fat phenotypes shown here are reported in Figure S3.
(D) $P_{daf\text{-}1}$*::daf-1::gfp* co-localized with $P_{tdc\text{-}1}$*::RFP* in RIM and RIC (white arrowheads).

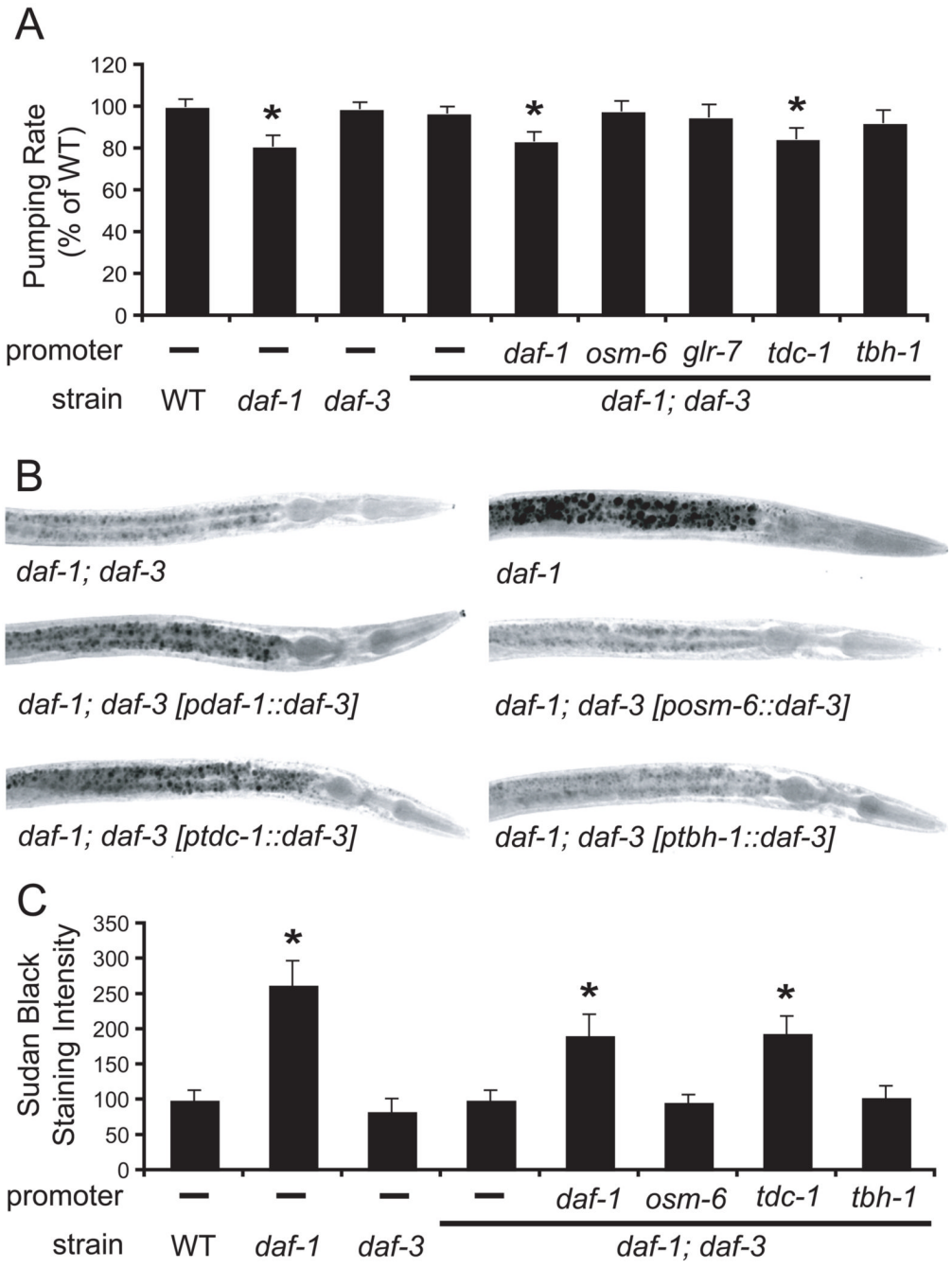

Figure 3. Activation of *daf-3* in RIM and RIC Causes Fat Accumulation despite Feeding Reduction

(A) Feeding rate. Asterisks indicate statistical significance ($p<0.001$ determined by ANOVA with Bonferroni post-test) relative to *daf-1(m40); daf-3(mgDf90)*. Standard deviation bars are shown.

(B–C) Fat content. Asterisks indicate statistical significance ($p<0.001$) as determined by t-test comparing genotype of interest with *daf-1(m40); daf-3(mgDf90)*. Standard error bars are shown.

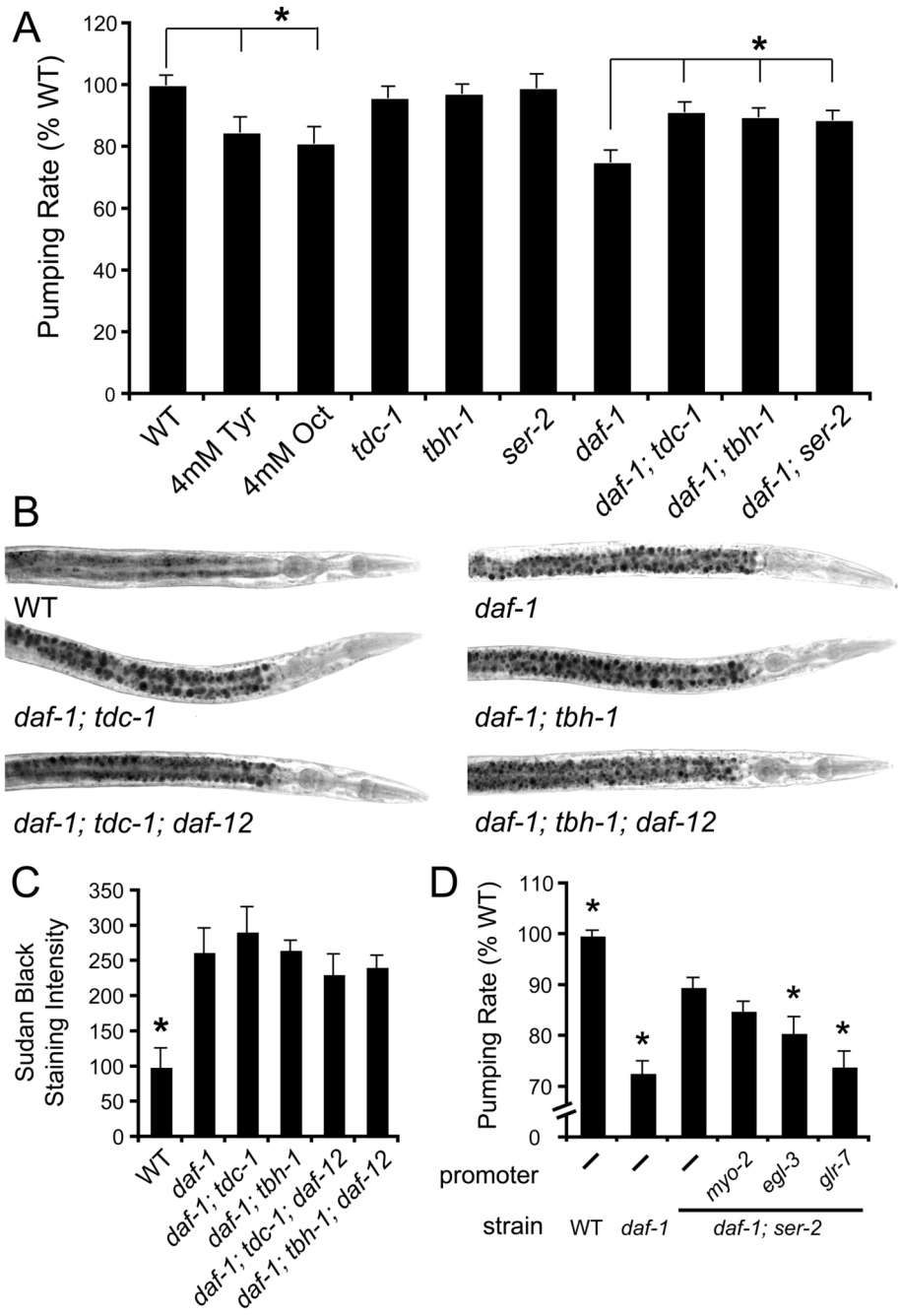

Figure 4. Tyramine and Octopamine Are Required for the Reduced Feeding Rate but not the Excess Fat of *daf-1(m40)* Mutants

(A) Effects of 4mM tyramine or octopamine on pumping rates of well-fed adult stage animals. Rescue of *daf-1(m40)* reduced feeding rate by each of *tdc-1(ok914)*, *tbh-1(ok1196)*, and *ser-2 (pk1357*). Asterisks indicate statistical significance ($p<0.001$ as determined by ANOVA with Bonferroni post-test) for indicated comparisons. Standard deviation bars are shown.

(B–C) *tdc-1(ok914)*, *tbh-1(ok1196)*, and *daf-12(m20)* mutations did not suppress the excess fat of *daf-1(m40)*. Asterisks indicate statistical significance ($p<0.001$) as determined by t-test comparing genotype of interest and *daf-1(m40)*. Standard error bars are shown.

(D) Reconstitution of SER-2 tyraminergic receptor using tissue specific promoters in *daf-(m40); ser-2(pk1357)* mutants. Asterisks indicate statistical significance ($p<0.001$ determined by ANOVA with Bonferroni post-test) relative to non-transgenic *daf-1(m40); ser-2 (pk1357).* Standard deviation bars are shown.

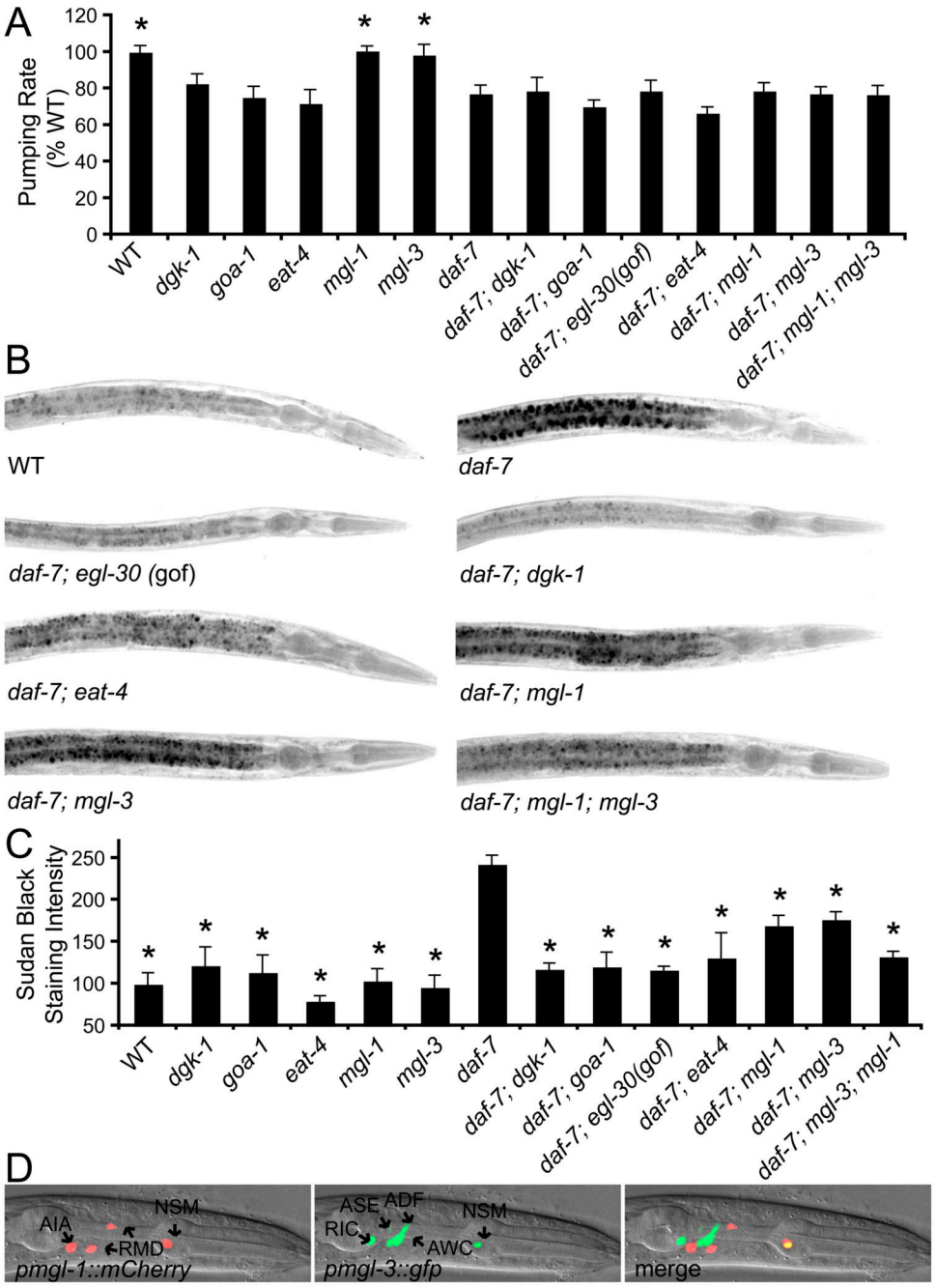

Figure 5. Mutations in GPCR Signaling and Metabotropic Glutamate Receptors Abrogate the Excess Fat but not Reduced Feeding of *daf-7(−)*.

Increased fat but not reduced feeding rate of *daf-7(e1372)* was suppressed by mutations in *goa-1*, *dgk-1*, *eat-4*, *mgl-1*, and *mgl-3* as well as a predicted gain of function mutation in *egl-30*.

(A) Feeding rate. Asterisks indicate statistical significance relative to *daf-7(e1372)* ($p<0.001$ determined by ANOVA with Bonferroni post-test). Standard deviation bars are shown.

(B) Representative examples of fat content in various mutants.

(C) Fat quantitations. Asterisks indicate statistical significance ($p<0.001$) as determined by t-test when comparing genotype of interest with *daf-7(e1372)*. Standard error bars are shown. (D) Expression sites of *mgl-1* and *mgl-3*. P_{mgl-1}*::mCherry* was expressed in AIA amphid interneurons, RMDV and RMDD ring interneurons/motoneurons, and pharyngeal NSM serotonergic neurons. P_{mgl-3}*::gfp* was expressed in NSM, ADF, ASE, and AWC amphid sensory neurons, and the RIB and RIC interneurons. Occasional expression in BAG ciliated neurons was also noted.

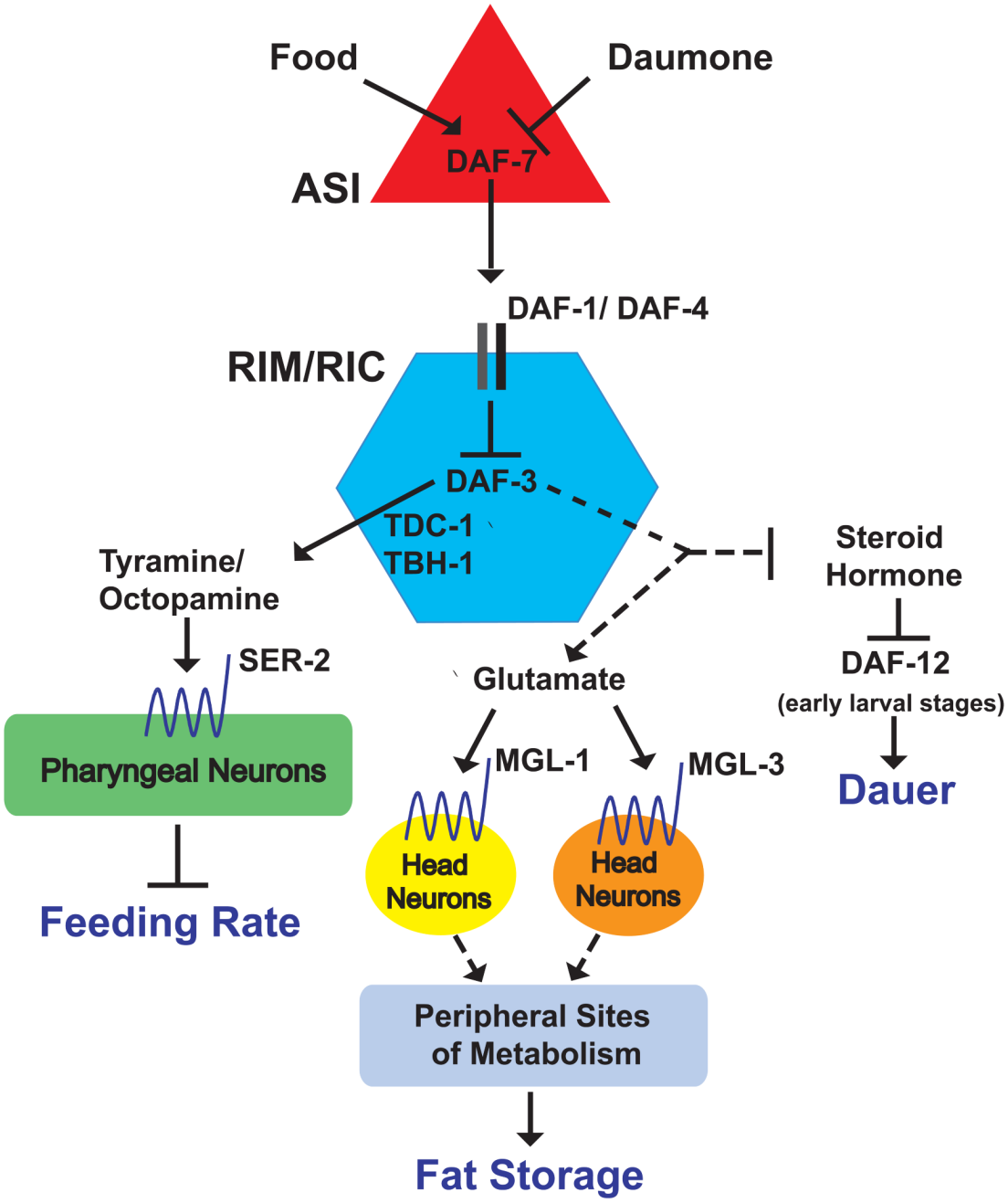

Figure 6. Model for the TGF-β Neural Circuit of Fat and Feeding Regulation

The DAF-7 TGF-β ligand expression is only detected in the ASI pair of sensory neurons while its receptors, DAF-1 and DAF-4 are broadly expressed in the nervous system. During favorable environmental conditions DAF-7 is secreted from ASI and signaling to two pairs of synaptically distant interneurons, RIM and RIC, to inhibit the DAF-3 co-SMAD. This promotes wild-type growth, egg laying, food intake behavior, and fat accumulation. Adverse environmental conditions such as increased population density combined with reduced food availability inactivate *daf-7*, relieving inhibition of DAF-3. During early larval stage, this leads to dauer formation and requires the nuclear hormone receptor DAF-12. In adults, DAF-3 activation in RIM and RIC causes reduced feeding rate, egg retention, and increased fat. These

processes are regulated through distinct signals. Subsequent to DAF-3 activation, tyramine, synthesized in RIM and RIC, and octopamine, synthesized in RIC, cause feeding reduction. Tyraminergic feeding reduction is mediated through activation of the SER-2 GPCR on a subset of pharyngeal neurons. Glutamate signaling through neuronally expressed metabotropic glutamate receptors, MGL-1 and MGL-3, mediates fat increasing effects of *daf-7(−)*. Fat increase is ultimately associated with increased *de novo* fat synthesis in the periphery.

Table 1

Expression of *daf-1* in Interneurons Is Sufficient to Rescue the Dauer Formation, Feeding Rate, and Fat Storage Phenotypes of *daf-1(m40)* Mutants

daf-1::gfp was expressed under various promoters in *daf-1(m40)* mutants. Larval dauer formation, adult feeding rate and fat content were measured in each of the transgenic lines. Indicated results were consistent for at least three independent transgenic lines. Promoters used to drive *daf-1::gfp* are grouped based on anatomical expressions.

	Genetic background	Promoter driving *daf-1::gfp*	No. of Cells expressing *daf-1::gfp*	% Dauer (n) [a]	% WT pumping rate [b]	Eggs retained[c]
Control	N2 (WT)	none		0 (150)	100 ± 2.8 [e]	+
	daf-1(m40)	none		98 (480)	76 ± 2.7	+++
	daf-1(m40)	*daf-1* [d]	many (>80) neurons	2 (179)	97 ± 2.1 [e]	+
Pan-Neuronal	*daf-1(m40)*	*egl-3* [d]	many (>80) neurons	3 (112)	98.2 ± 3 [e]	+
Sensory Neurons	*daf-1(m40)*	*bbs-1*	60 ciliated neurons	99 (142)	75 ± 6.7	+++
		osm-6	56 ciliated neurons	100 (140)	69 ± 3.5	+++
		daf-7	2 (ASI)	100 (79)	N/D	+++
Pharynx	*daf-1(m40)*	*glr-8*	25 pharyngeal neurons and interneurons	56 (147)	81.7 ± 4	+++
		glr-7	9 pharyngeal neurons	98 (249)	71 ± 6.0	+++
		B0280.7	5 pharyngeal gland	98 (181)	74 ± 5.4	+++
Interneurons	*daf-1(m40)*	*glr-2*	24	94 (332)	74 ± 2.3	+++
		unc-47	29	100 (102)	72 ± 4.7	+++
		unc-17	80	37 (174)	76 ± 6.3	+++
		glr-5 [d]	56	6 (175)	97 ± 1.9 [e]	++
		glr-4 [d]	38	3 (248)	96 ± 2.9 [e]	++
		glr-1 [d]	24	14 (170)	90 ± 4.6 [e]	++
		ggr-1	10	94(119)	77 ± 7.1	+++
		flp-1	2	100 (216)	76 ± 2.6	+++
		dop-1	12	100 (231)	76 ± 6.1	++
		nmr-2 [d]	12	2 (221)	95 ± 3.2 [e]	++
		tdc-1 [d]	4 interneurons and UV1 cells	1 (188)	98 ± 3.1 [e]	++
		tbh-1 [d]	2	57 (178)	84 ± 3.1 [e]	++

[a] % animals that entered dauer when placed on food plates as L1s at 25°C. Phenotypic example shown in Figure S1

[b] Average pumping rate of well-fed, young gravid adults. Standard deviations are shown.

[c] Young, well-fed wild-type animals retained ~10 eggs on average. This phenotype is denoted as (+). Mutants such as *daf-1(m40)* retained excess eggs (~24), denoted as (+++). Intermediate egg retention is denoted as (++). Phenotypic examples are shown in Figure S1.

[d] Expression of *daf-1(+)* by these promoters reduced the excess fat of *daf-1(m40)* to wild-type levels. Phenotypic examples shown in Figure 1B.

[e] Statistically significant ($p < 0.001$, determined by ANOVA with Bonferroni post-test) increases in feeding rate relative to *daf-1(m40)*.